Atomic Energy of Canada Limited

AN INTENSE NEUTRON GENERATOR BASED ON A PROTON ACCELERATOR

by

G A. BARTHOLOMEW, J.C D MILTON and E W VOGT

Chalk River, Ontario

August, 1964

AECL-2059

An Intense Neutron Generator Based on a Proton Accelerator

August 1964

This report summarizes the conclusions of the High Flux Neutron Facility Study Committee which functioned during the winter of 1963-1964.

AECL-2059

Committee Members:-

G.A. Bartholomew (Chairman)
M. Bercovitch
B.G. Chidley
R.L. Clarke
G. Dolling
T.A. Eastwood
G.T. Ewan
J.S. Fraser
J.W. Knowles
G.E. Lee-Whiting
J.C.D. Milton
A. Pearson
O.J.C. Runnalls
I.M. Thorson
P.R. Tunnicliffe
E.W. Vogt
A.D.B. Woods
A.H. Wilson (Secretary)
H.H. Clayton (Observer)
G.C. Hanna (Observer)
S. Kushneriuk (Consultant)

Editors:-

G.A. Bartholomew
J.C.D. Milton
E.W. Vogt

ABSTRACT

A study has been made of the demand for a neutron facility with a thermal flux of $\geq 10^{16}$ n cm^{-2} sec^{-1} and of possible methods of producing such fluxes with existing or presently developing technology. Experimental projects proposed by neutron users requiring high fluxes call for neutrons of all energies from thermal to 100 MeV with both continuous-wave and pulsed output.

Consideration of the heat generated in the source per useful neutron liberated shows that the (p,xn) reaction with 400-1000 MeV bombarding energies and heavy element targets (e.g. bismuth, lead) is capable of greater specific source strength than other possible methods realizable within the time scale. A preliminary parameter optimization carried through for the accelerator currently promising greatest economy (the separated orbit cyclotron or S.O.C.), reveals that a facility delivering a proton beam of about 65 mA at about 1 BeV would satisfy the flux requirement with a neutron cost significantly more favourable than that projected for a high flux reactor. It is suggested that a proton storage ring providing post-acceleration pulsing of the proton beam should be developed for the facility. With this elaboration, and by taking advantage of the intrinsic microscopic pulse structure provided by the radio frequency duty cycle, a very versatile source may be devised capable of producing multiple beams of continuous and

pulsed neutrons with a wide range of energies and pulse widths. The source promises to be of great value for high flux irradiations and as a pilot facility for advanced reactor technology. The proposed proton accelerator also constitutes a meson source capable of producing beams of π and μ mesons and of neutrinos orders of magnitude more intense than those of any accelerator presently in use. These beams, which can be produced simultaneously with the neutron beams, open vast areas of new research in fundamental nuclear structure, elementary particle physics, and perhaps also in biology and medicine.

TABLE OF CONTENTS

1. OUTLINE OF STUDY AND PROPOSALS

1.1 Purpose of Study

The success of the research programs using reactor neutrons at Chalk River Nuclear Laboratories has depended in large part on the very high fluxes and excellent beam tube facilities available in NRX and NRU reactors. Although the NRU reactor is still today a leading research facility, there can be little doubt that it will soon be surpassed. In Table I, Appendix 1, a comparison is made between the characteristics of NRU as a neutron beam research reactor and those of the HFBR reactor[1,2], now nearing completion at Brookhaven and the Argonne AARR reactor[3,4]. The discussion below of possible experiments in solid state physics and nuclear structure to be carried out with such high flux facilities shows that these devices promise to contribute greatly to fields pioneered at Chalk River. It is then clear from the comparison of Table I, Appendix 1, that in a few years time, it will be desirable to have a facility with thermal fluxes in beam tubes considerably in excess of 10^{15} cm^{-2} sec^{-1}.

The purpose of the present study is to seek a practical neutron facility, realizable in the next ten years, which would deliver the highest possible flux for neutron experiments. In order to constitute a significant step forward, it was considered that the thermal flux should be at least 10^{16} cm^{-2} sec^{-1}, representing roughly a 60-fold increase over the flux in an NRX through tube ($\sim$ 160-fold over that in a reentrant thimble) and an 8 to 14-fold increase over the beam tube fluxes of the research reactors now under construction or consideration.

1.2 Proposed Experiments and Requirements For High Flux

A summary of experiments proposed by neutron users for a high flux facility is given in Appendix 2. This summary shows that the primary need is for thermal neutrons. Many of the experiments requiring thermal neutrons would benefit if the neutron source were pulsed, although for some the advantage is not large. On the other hand, a number of experiments require epithermal, resonance or fast neutrons and many of these would benefit greatly from pulsing at the source. It is desirable to satisfy as many of these requirements as possible consistent with the primary demand for thermal neutrons.

1.3 Type of Facility

The continuous production of thermal neutrons at higher fluxes in a reactor is limited ultimately by the difficulty of removal of heat from the fuel elements and the cost of the fuel. Any other device faces similar problems but may gain relative to a reactor in producing less heat per neutron and in avoiding various restrictions imposed by criticality. Appendix 3 considers various devices that may realize these improvements, including fusion and high energy and low energy accelerators of various kinds. It is concluded that in the time scale envisaged the only practicable method of generating continuous fluxes of thermal neutrons in the range $\geqslant 10^{16}$ cm^{-2} sec^{-1} is by high current, high energy proton bombardment of a heavy target, e.g. bismuth, surrounded by a heavy water moderator. By this method, it is possible in principle to liberate in the target as little as 23 MeV per escaping neutron, some 8 times less than the energy deposited per neutron in a uranium rod in a reactor. A factor of approximately two, in the ratio of flux to neutron source strength, may be gained from the geometry and neutron absorption properties of the target relative to that of a reactor core. Until recently a central problem with accelerators has been the production of sufficient beam power to realize this potential gain. A further problem for a high power accelerator concerns the reduction of the electrical power bill, which is the principal operating cost.

Among the various possible high power proton accelerators being considered today (Table II, Appendix 4), the Separated Orbit Cyclotron (S.O.C.) presently appears, for reasons of size, cost, and economy of operation, to be the most promising. A brief description of this accelerator and a discussion of the advantages and disadvantages of the design are given in Appendix 4.

1.4 A Possible S.O.C. High Flux Facility

1.4.1 Basic Design; Continuous Thermal Neutrons

The determination of the current and voltage parameters of the accelerator to give the most economical production of neutrons at a given flux depends fundamentally on (1) the neutron yield per proton as a function of the energy for protons incident on a target or given material, (2) the dimensions of the target and moderator, (3) the heat dissipation capability of the target, and (4) the details of the capital and operating cost of the accelerator as a function of current and voltage. A preliminary design and cost optimization calculation in Appendix 5 gives the following parameters for a continuous source:

A. Source geometry, as shown in Fig. 1:

Target: Bi, radius 5 cm, length 60 cm.
Moderator: D_2O, length 300 cm, radius 125 cm.

B. Accelerator Parameters:

Energy 970 MeV, current 65 ma., R.F. frequency 200 Mc/sec

Beam Power	63	MW
Cavity Power (S.O.C. plus injector)	13	MW
Total R.F. Power	76	MW
Magnet Power	3	MW
Total line power (assuming 60% 60 cycle to R.F. efficiency)	130	MW
Target dissipation	36	MW or 8 MW/litre

Neutron Output:

Source strength	9×10^{18} sec^{-1}
Midplane thermal flux at 17 cm radius	10^{16} cm^{-2} sec^{-1}

C. Capital Costs:

Accelerator	~ \$40 M
Building, D_2O, Electrical, Service Areas, Research equipment and 20% contingency	~ \$25 M
Total (excluding engineering design costs)	~ \$65 M

The accelerator cost (main item, R.F. power equipment) is roughly proportional to beam current and hence neutron flux. It would be feasible to begin at reduced current with provision for subsequent increases to full power.

D. Operating Costs:

Power bill at \$35/kW year	\$ 4.5 M
Other costs	~ \$ 3 M
	~ \$ 7.5 M

E. Comparison with hypothetical high flux reactor operated in Canada, Power: 40 MW, Flux: 7×10^{14} cm^{-2} sec^{-1} (similar to HFBR)

	S.O.C. \$M	Reactor \$M
Capital cost per 10^{14} cm^{-2} sec^{-1} flux	0.65	1.7
Capital cost per 10^{18} sec^{-1} source strength	7.2	10.
Annual operating cost per 10^{14} cm^{-2} sec^{-1} flux	0.062	0.22
Cost of neutrons (operating costs only) per gram	0.013	0.029

1.4.2 Modifications to Provide Pulsed Neutron Sources

It would appear to be feasible to take advantage of the microscopic bunching of the beam imposed by the R.F. duty cycle to produce short neutron pulses ($\leq 10^{-8}$ sec) for resonance and fast neutron experiments.

It would also be very desirable to couple a storage ring to the output of the S.O.C. as shown in Fig. 2. The storage ring would act as a 'buncher' converting the continuous proton beam into bursts of short duration and high intensity. Ideally the burst length would be about 10^{-7} sec and the repetition rate 200 pps. The pulsed neutron source produced by such a beam would provide excellent facilities for thermal, epithermal, and resonance neutron experiments. The storage ring, realization of which would probably involve considerable development work, would not be essential initially and could be added to the facility later.

Further details of both pulsing modes is given in Appendix 6.

1.5 Advantages of Proton Accelerator Neutron Facility

The present study shows that the accelerators currently being designed for high energy physics, such as those listed in Table II, Appendix 4, may form the basis for development of neutron generators of the next stage beyond reactors. This is particularly true when the storage ring is included as a pulse facility. The complete neutron generator shown schematically in Figure 3 would represent a unique facility unmatched at any present laboratory. Among the attractive features of this device are the following:-

1.5.1 Operational Advantages

The proton accelerator is superior to a reactor as a neutron source in the following ways:-

(a) The site of neutron production in the accelerator system is not an integral part of the plant and therefore may be more accessible for modification or replacement than the core of a reactor. Targets of different design and different purpose can be installed at will.

(b) The neutron source can be made to provide a wide range of neutron spectra simply by changing the size and shape of the moderator. It is possible to have both a continuous and a pulsed source. Fast and thermal pulsing can be accomplished concurrently.

(c) The target presents no criticality problems. Furthermore, since the beam probably can be shut off in microseconds, catastrophic heating of the target resulting from coolant failure should be avoidable.

Furthermore, the target is not consumed, as in a fissile fuel; the spallation products are not very different from the parent material in their neutron production properties, though they may have larger thermal capture cross sections.

(d) It is possible to have two or more complete target areas separated and shielded from each other so that changes of target or apparatus could be carried out at one while experiments were in progress at the others. A possible layout of target space is discussed in Appendix 7.

1.5.2 <u>Operational Disadvantages</u>

Among disadvantages presented by the accelerator are the following:-

1. Experimenters would have to contend with an intense background of high energy neutrons, mesons and γ-rays from the target. These can be circumvented to a large extent by the use of tangential beam tubes which do not look directly at the target. However, it is likely that special precautions to prevent undesirable activation of experimental equipment exposed to the fast neutron flux will be necessary (Appendix 7).

2. The health hazard created by the high energy particles is formidable and very thick shielding (up to 35 ft. of concrete) will be necessary to protect personnel, (Appendix 7).

3. The region of peak flux around the target is small, (1-2 feet circum by 2 feet long), compared to the NRU core (32 feet circum by 10 feet long) and presents difficulties in accommodating a large number of beam tubes in high flux positions.

1.5.3 Additional Advantages for Research

In addition to satisfying the various requirements for neutron experiments and for production of radioactive isotopes, the accelerator opens up several other fields of research.

1.5.3.1 Advanced Nuclear Power Technology

The development of a feasible cycle for uranium or thorium burning or a process for producing fissile materials using high energy bombardment of heavy element targets[5,6] will require an exhaustive study of the neutron yield and the heat generation in such reactions. Initial studies involving deuteron acceleration were carried out as part of the Livermore Radiation Laboratory MTA project[6]. Further studies of these questions would become possible with a high current high energy proton accelerator.

1.5.3.2 High Energy Physics

An enormous field of fundamental research can be tapped with the intense beams of high energy protons, neutrons, π^+, π^-, μ^+ and μ^- mesons and ν_μ, $\bar{\nu}_\mu$, ν_e, $\bar{\nu}_e$ neutrinos of various energies available from such an accelerator. In the field of nuclear structure intense beams of π and μ mesons may provide new means of probing the nucleus, comparable in power to the beams of neutrons, protons or electrons now available. A summary of some suggested experiments in this new field and in the field of high energy particle physics is given in Appendix 8.

1.5.3.3 Biology and Medicine

A study of the experiments in biology and medicine that would be possible with the various high energy beams has not been made in the present survey. We draw attention, however, to a recent discussion of isodose distributions for 50 MeV π^- mesons by the

Oak Ridge group[7] which shows that the π mesons provide a means of tissue irradiation far superior to Co^{60} γ-rays or 110 MeV protons. Other interesting applications of these beams in biological research will no doubt be found.

2. DISCUSSION

The neutron generator is a versatile facility with considerable latitude for future expansion or modification. It may be feasible for example to increase the current to several hundreds of milliamps. It may also be possible to increase the beam energy by adding further rings to the spiral of the S.O.C., by adding additional spirals, or by adding some other high energy device. Conversely, it would not be essential to begin with the complete installation if savings of capital outlay were necessary. For example, it may be considered advisable to begin with only one neutron target room and omit the other together with the meson research area. As mentioned above, the storage ring might also be omitted initially.

The construction of the neutron facility would give impetus to research and development in many fields. The scope of such a device in solid state, nuclear, and high energy physics, as well as the more applied fields of reactor physics and nuclear engineering, has already been discussed. The new skills and technology learned during the development and construction stages of the project would also bring direct benefits to many branches of industry.

FIGURE CAPTIONS

Figure 1 - Schematic view showing dimensions of Bi target and D_2O moderator for continuous operation.

Figure 2 - Schematic arrangement of S.O.C. accelerator, storage ring and target. The S.O.C. consists of a 15 MeV Linac injector and two high energy stages 15-120 MeV and 120-970 MeV.

Figure 3 - Schematic arrangement of complete neutron facility showing S.O.C. accelerator with concentric storage ring, 100-300 MeV short pulse area, meson experimental area, two neutron source areas, and finally a proton irradiation room. The shielding between the neutron areas and between these areas and other areas is heavy concrete. The neutron target assembly is shown in more detail in Fig. 7.1.

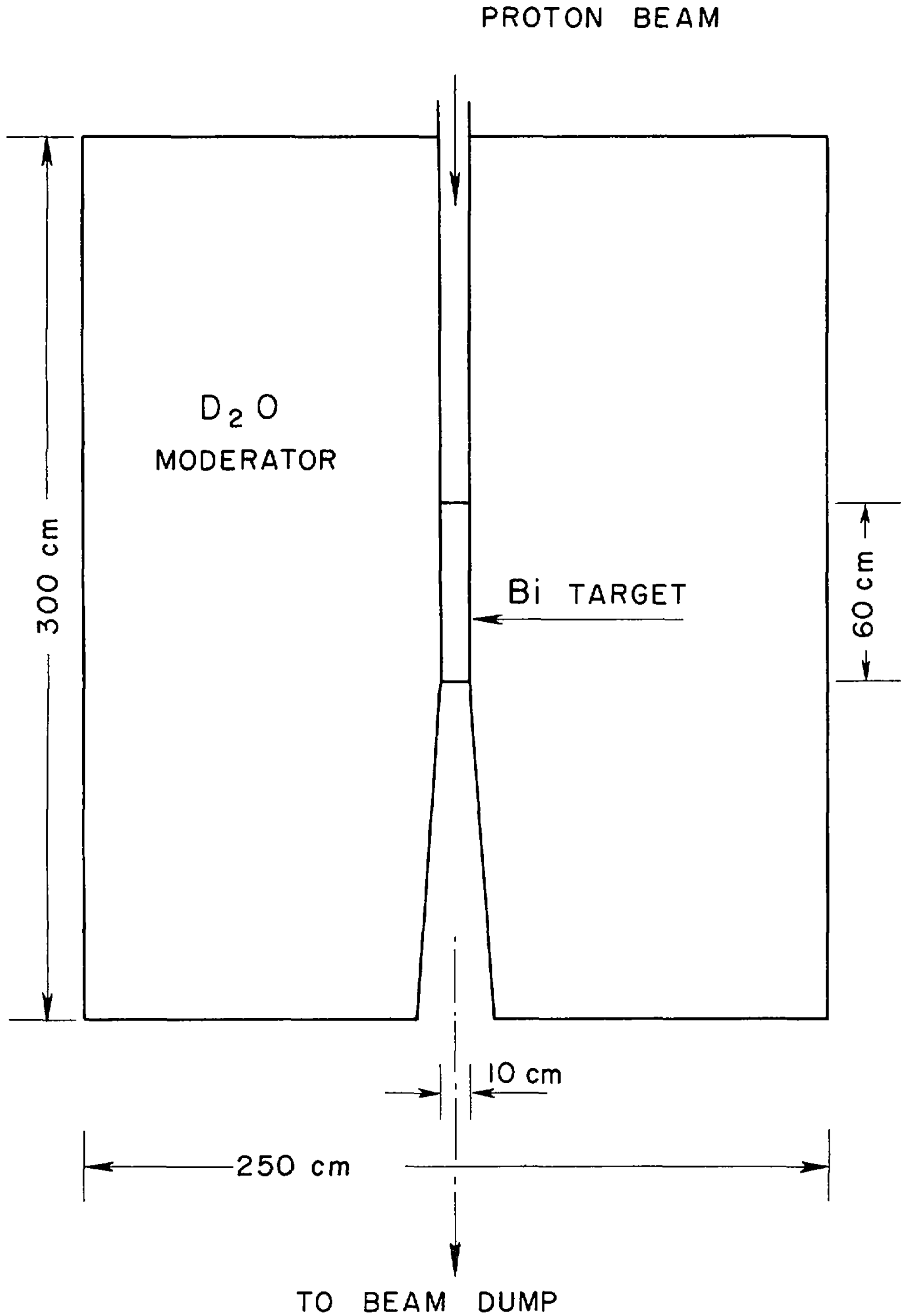

FIG. I TARGET AND MODERATOR ASSEMBLY

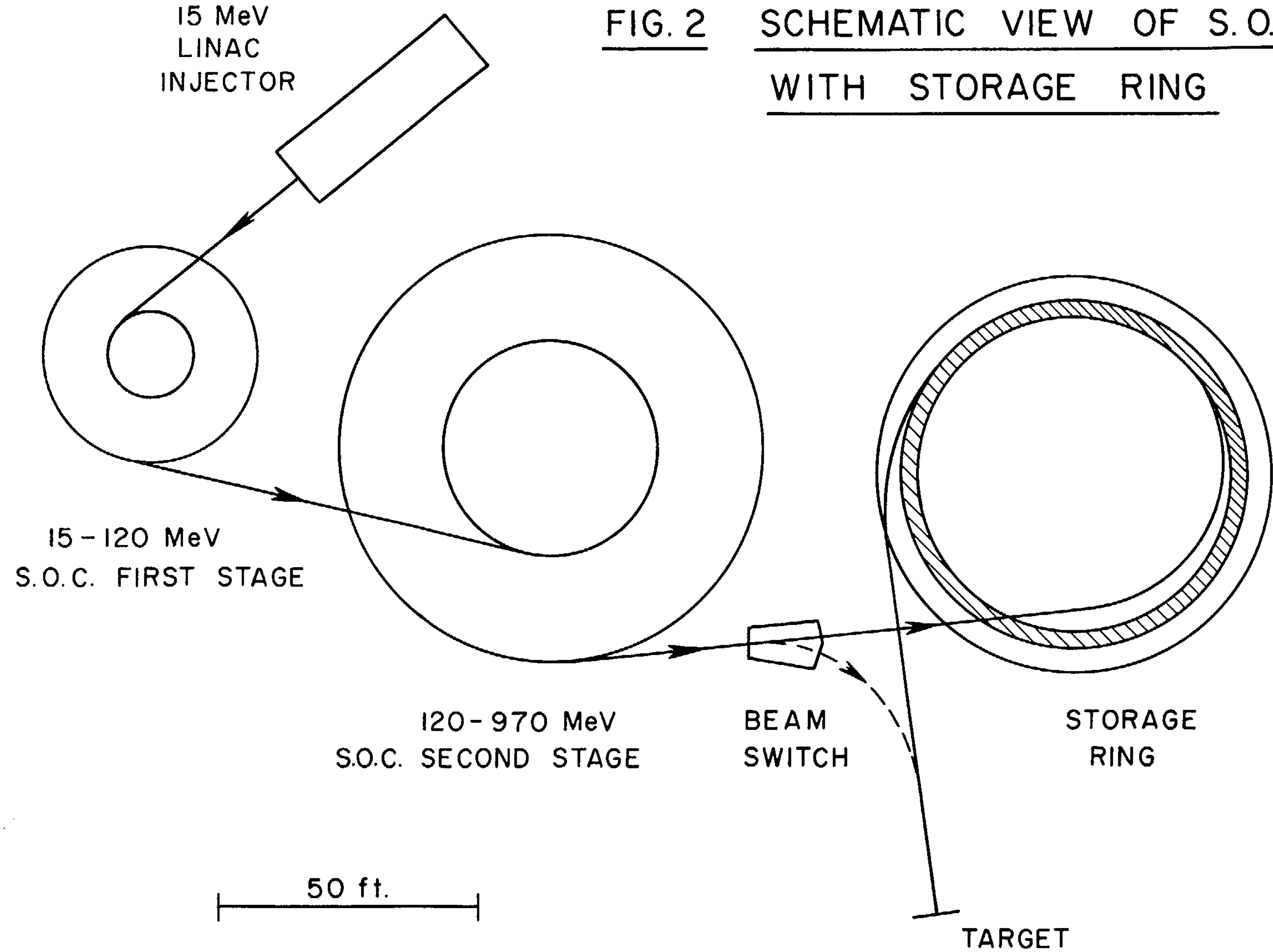

FIG. 2 SCHEMATIC VIEW OF S.O.C. WITH STORAGE RING

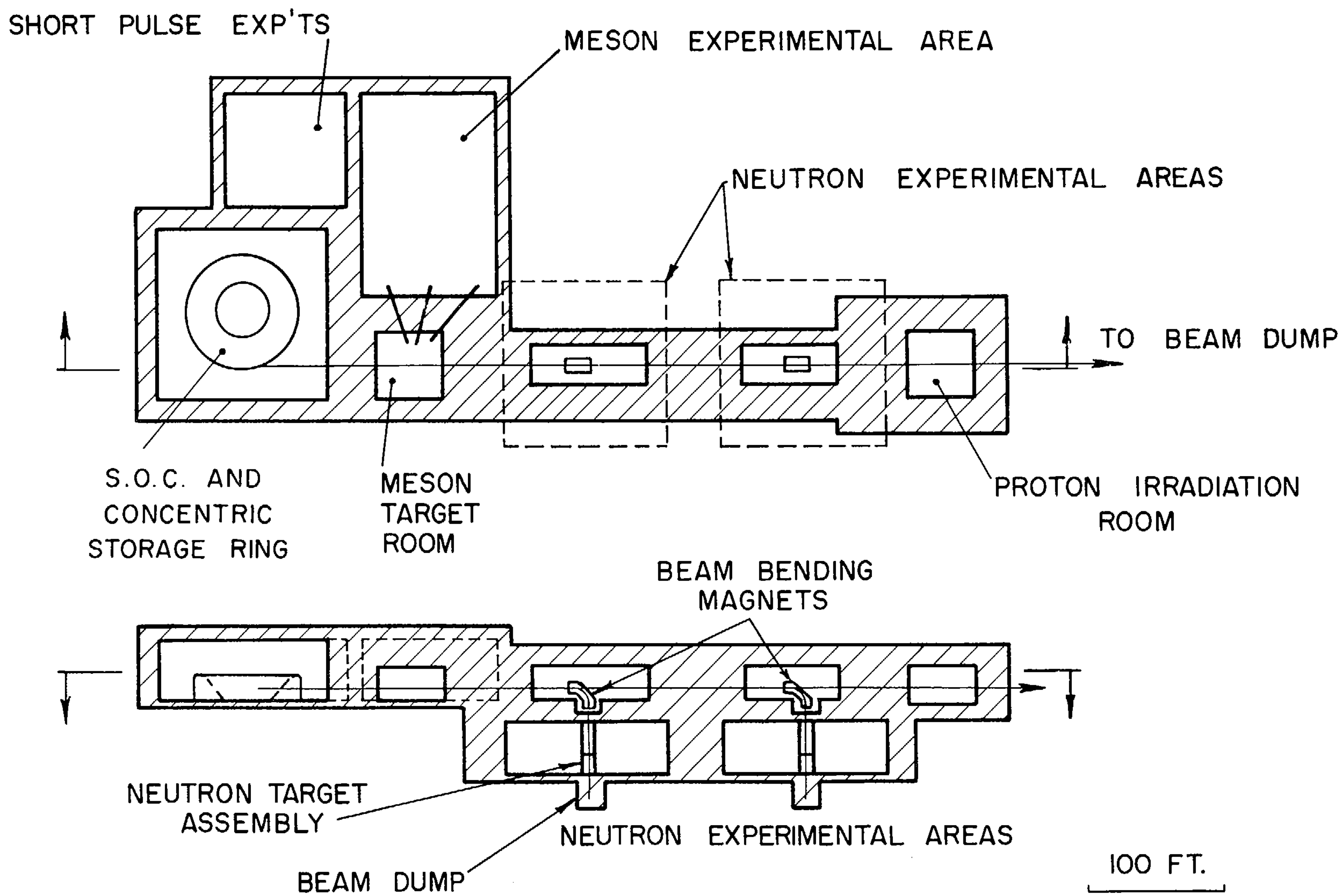

SOC ACCELERATOR & TARGET AREA

FIG. 3

3. APPENDICES

3.1 Appendix 1

Comparison of Parameters and Facilities of Research Reactors

In Table I a comparison is made between the characteristics of NRU as a neutron beam research reactor and those of the HFBR reactor, now nearing completion at Brookhaven and the Argonne Reactor, AARR. The latter reactors were planned primarily for neutron beam research and possess a number of highly desirable features such as a good thermal to fast neutron ratio afforded by many tangential holes, and beam holes 'tailored' for special purposes, e.g. for the production of beams of cold neutrons. Several other 'modern generation' reactors with fluxes exceeding that of N.R.U. but with somewhat less attractive beam facilities than those in Table I are reviewed in a recent article by Cole and Weinberg[8].

3.2 Appendix 2

Neutron Users' Requirements for High Neutron Flux

A summary of experiments that would be possible with a flux up to 100 times that of NRU has recently been made by neutron users at CRNL and is given in section 3.2.2 below.

3.2.1 Required Characteristics of Neutron Source

Several conclusions may be drawn from this study which clarify the characteristics that a generally useful neutron source should possess. The requirements of various types of experiment for neutron energy and pulse structure are displayed in Fig. 2.1. The limits of the regions shown on this diagram should be interpreted as illustrative demarkations only and not as precise or final boundaries.

3.2.1.1 Energy Requirements

The spectrum of neutron energies required for various experiments ranges from thermal or subthermal neutrons (≤ 0.1 eV) through the epithermal and resonance regions to fast neutrons with energies $\underset{\sim}{\ }$ 100 MeV. It is necessary therefore that the source should be capable of providing beams of neutrons over a wide range of energies and that as many as possible of these beams should be available simultaneously.

3.2.1.2 Pulse Structure Requirements

The requirements for pulsing are also varied. In considering advantages and disadvantages of pulsing it was assumed

TABLE I

Comparison of Parameters and Horizontal Beam Tube Facilities for Research Reactors

Parameters	HFBR [a]	AARR [b]	NRU (new loading)
Power MW	40	100	60
Core and Fuel	Compact U^{235}-Al Alloy	Compact, central H_2O island Al-$U_3^{235}O_8$	distributed U^{235}-Al Alloy
Moderator	D_2O external	H_2O trap	D_2O in lattice
Reflector	D_2O	Be	H_2O
Primary cooling	D_2O	H_2O	D_2O
Max. beam tube flux $\times 10^{15}$ cm^{-2} sec^{-1}	0.7	1.3 (4.9 in island)	0.16 (through tube) 0.06 (reentrant tube)
Beam tubes:			
(a) Horiz. radial	1(8.9 cm)	12(10.8 cm and elliptical)	4(30.4 and 15.2 cm re-entrant)[c]
(b) Horiz. tangential	7(8.9 cm)		2(30.4 and 15.2 cm in TC)
(c) through		2(10.8 cm)	2(8.2 x 11.4 cm elliptical)
(d) cold neutron	1(30.5 cm)		
(e) thermal column			2(30.4 and 15.2 cm through) 5(61,30.4 and 17.1 cm)
	9	14	15

a.- See reference 1 and 2
b.- See references 3 and 4
c.- There are an additional 5(15.2 cm) and 1(30.4 cm) radial holes stopping at the reflector which have very low flux and are not used.

FIG. 2·1 ENERGY AND PULSE LENGTH REQUIREMENTS

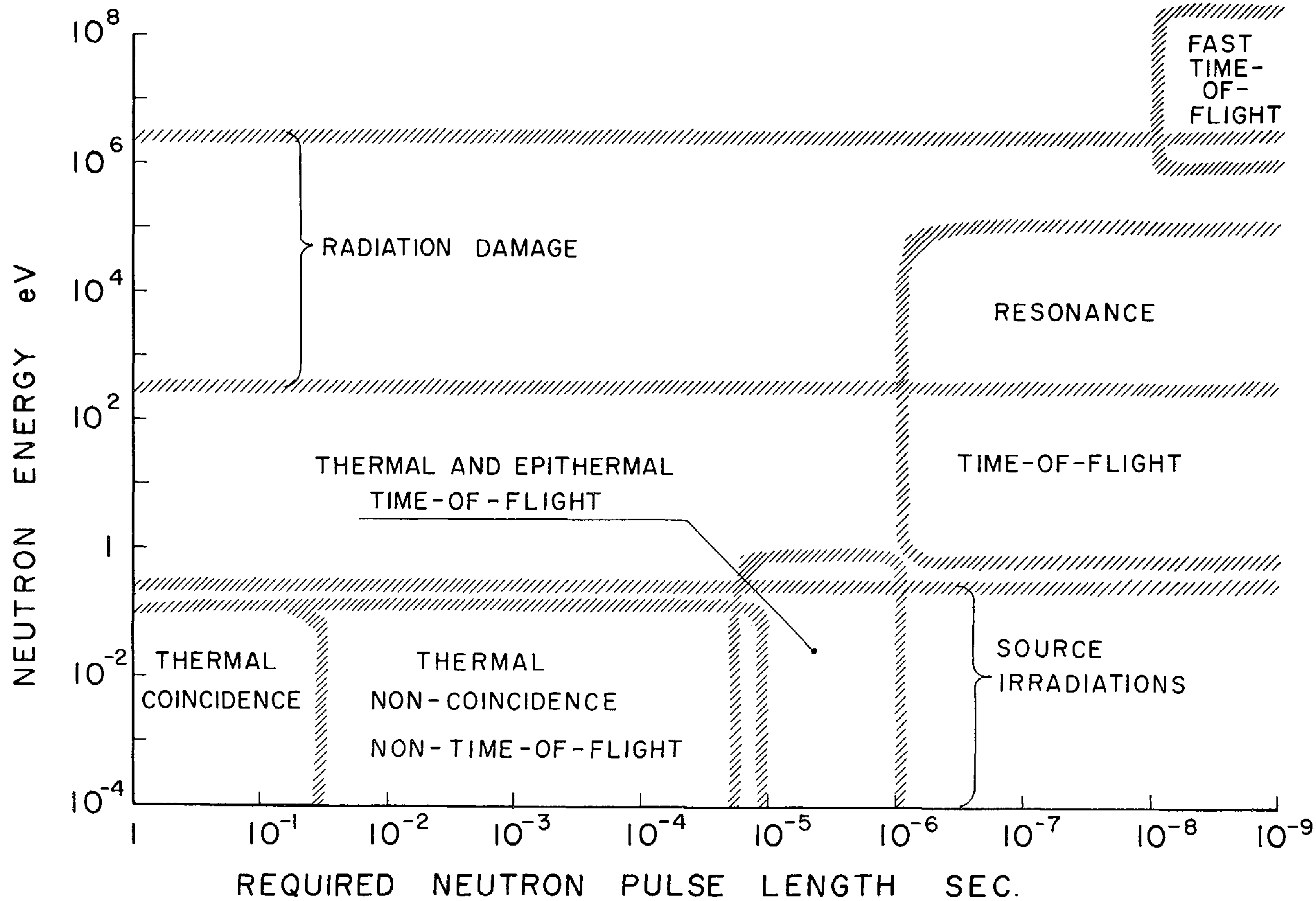

by the users that the time averaged neutron flux would remain constant regardless of the pulsing conditions. The requirements for pulsing may be classified in four categories.

A. Experiments independent of pulse structure. These comprise the radiation damage and irradiation type of experiments.

B. Experiments that are possible only if the source is pulsed. These are fast neutron time-of-flight experiments requiring very short pulses that are difficult to produce by chopper techniques.

C. Experiments for which a pulsed source may introduce a definite disadvantage. In this category are certain multiple coincidence experiments that would suffer from excessive random coincidence background counting rates if the events were concentrated in bursts of high intensity. Experiments employing counters suffering from dead time or overload effects at very high counting rates also fall in this category.

D. Experiments that could be carried out with a continuous source but would, nevertheless, benefit from pulsing. This category may be further subdivided into two groups.

(1) Time-of-flight experiments that are normally carried out at a reactor with pulsing provided by some form of chopper. For some of these experiments if would be necessary for reasons of time definition to retain some or all of the chopper systems with a pulsed source. However, with a synchronized pulsed-source and chopper arrangement it may be possible substantially to reduce

backgrounds arising from unwanted radiations in the beam and from scattered 'room' radiation.

(2) Direct counting (non-coincidence) spectrometer-type experiments. Here also a considerable reduction of continuous 'room' background and some time-dependent background from the beam may be achieved if the detector is gated-on in synchronism with the neutron pulses and gated-off between pulses.

An important practical disadvantage of pulsing is the considerably greater complexity of both mechanical parts and recording equipment usually associated with a time-dependent counting system as compared to a continuous system. The experimental time saved by improving the signal-to-noise ratio with a pulsed system must therefore be balanced against the longer time required to get such a system into operation and the inevitably greater maintenance time. For some experiments the advantages of pulsing may not be very large. On the other hand it may be shown that for experiments with very low counting rate, where 'room' background is a limitation, pulsing is always advantageous for improving the signal-to-background ratio.

3.2.2 Survey of Proposed Experiments

3.2.2.1 Solid State and Scattering Law Experiments

Many new and interesting experiments would be possible with a 100 times greater flux; representative examples are discussed below.

A. Thin Specimens

(a) Determination of phonon dispersion relations in materials where only small samples are available.

(b) Determination of antiferromagnetic spin wave dispersion relations for various rare earths.

(c) Determination of the time-dependent pair correlation function for liquid He^3.

(d) Studies of neutron diffraction in the presence of strong extinction effects.

B. High Resolution

(a) Study of anharmonic effects especially at low temperatures.

(b) Study of effect of superconductivity on normal vibrations in a crystal.

(c) Study of small discontinuities and other singularities in the phonon dispersion relation of a metal (e.g. the Kohn effect).

C. High Energies

(a) Extension to larger momentum and energy transfers of the partial differential scattering cross-section measurements on moderator materials to remove the present rather heavy dependence on detailed models for the cross section in the energy transfer region $\Delta E = 0.15$ to 0.40 eV.

(b) Studies of the dispersion relations for relatively high energy transitions such as optical modes in some single crystals (e.g. $SrTiO_3$ or diamond) or spin waves in metals.

D. Polarization

Analysis of polarization as well as energy distributions following scattering of a polarized initial beam.

3.2.2.2 Fission

The increase of neutron fluxes by two or more orders of magnitude would benefit fission studies by permitting thinner sources and better statistics in the region of symmetric fission, by facilitating use of very pure (low background) thermal beams and by making possible extension of existing experiments to the epithermal and resonance region.

A list of some possible fission experiments follows:

A. Primary Charge Division could be studied by several different methods.

(a) By precision determination of the X-rays emitted by the fission fragments stopped in an absorber or emitted following the internal conversion of a prompt γ-ray. The X-rays could be measured with a curved crystal X-ray spectrometer or with recently developed p-i-n detectors.

(b) By measurement of Auger electrons from the source or stopping fragment. A suitable detector would be a high transmission β-spectrometer such as the "orange" spectrometer.

(c) By β-counting in conjunction with a mass separator.

B. Angular Momentum of the Fragments

Multiple coincidence methods (n-n-f, n-γ-f, and n-f-f), all with very low counting rate and requiring very pure beams, provide possible ways of studying fragment angular momentum.

C. Partial Fission Cross Sections

Measurements of partial cross sections in the resonance region are of interest for elucidation of the question of fission channels.

D. Spin Determinations for Fission Resonances

E. Polarized Neutron and Target Studies

F. Studies of the level schemes of neutron rich nuclei by observing the γ spectra of the fragments in high resolution p-i-n detectors. Many such nuclei are conveniently produced only as fission fragments.

3.2.2.3 <u>Neutron Capture γ-Rays</u>

A. Resonance Capture γ-Ray Experiments

The increased flux would permit high resolution spectroscopy (with lithium drifted germanium detectors) over a wide energy range in the resonance region. Spin measurements by γ-γ correlations and neutron-γ-ray angular distributions would also be possible at many resonances.

B. Thermal Capture Experiments

Among experiments which would fall well within the realm of feasibility are:

(a) Measurement of multipolarities of γ-rays by internal conversion coefficient or internal pair electron correlation measurements.

(b) Extension of measurements of circular polarization of γ-rays following capture of polarized neutrons to all parts of the primary spectrum. These experiments lead to information concerning spins of levels and γ-ray multipolarities.

(c) Resonance scattering experiments of the type where the energy deficit is supplied by recoil from a previous capture γ-ray. Such experiments yield information on the mean lives of γ-emitting states.

(d) Resonance scattering of radiations selected from a white spectrum by crystal diffraction could be used for lifetime determinations and for γ-γ angular correlation measurements over a wide range of excitation energies.

(e) Resonance scattering of both γ-rays and neutrons in the forward direction from single crystal samples could be used to measure the width and shape of nuclear resonances.

3.2.2.4 Reactor Physics Experiments

Among experiments in this field which would benefit from an increased flux, $> 5 \times 10^{15}$ cm^{-2} sec^{-1}, are the following:

A. Measurement of cross sections of short-lived precursors, including isomers, of stable or long-lived fission products.

B. Yield Measurements of known short-lived high-cross-section fission products by measuring, in the Chalk River Pool Test Reactor

(P.T.R.), the reactivity changes with time in irradiated fuel or chemically separated fractions thereof.

C. A search for fission products of the same characteristics as B, but as yet unidentified, using a combination of chemical separation and P.T.R. swing techniques.

D. Measurement of direct fission yields for nuclides shielded by relatively short-lived precursors and accumulated yields for short-lived nuclei not at present accessible.

E. With a relatively pure thermal flux of $1 - 5 \times 10^{14}$ cm^{-2} sec^{-1} and Westcott $r < 10^{-4}$, cross sections of nuclei with relatively large resonance neutron contributions and/or markedly non 1/v energy variations could be measured by irradiation to high burnup followed by mass analysis.

F. With a high intensity pulsed source it would be possible to make differential measurements of the neutron spectra in energy and time following the introduction of a fast neutron pulse into a finite crystalline or a liquid moderator. In addition, the effect of the energy variation of coherent elastic scattering cross sections on preferential neutron energy leakage in crystalline moderators could be studied.

G. Study of U and Th target assemblies for production of fissile material or power.

3.2.2.5 Preparation of Radioactive Materials

A. Decay scheme studies: An n-fold increase in flux results in proportionate increase of the quantities of short-lived species that are available for study. The yields of p-th order capture reactions go as n^p. An increased flux would make available new species for decay studies in the lower part of the table. In the transuranic region it may even be possible to manufacture new elements.

B. Production of tracers in a higher flux would make possible many new experiments not now possible.

C. Independent fission yield measurements and yield measurements in the valley or on the wings of the mass yield curve using either radiometric or mass spectrometric methods could be done more accurately.

D. Production of very high specific activity sources for special uses, e.g. thermoelectric power sources in space.

3.2.2.6 Radiation Damage Studies

An increase of a factor of ten in the fast flux available would be very advantageous for low temperature radiation damage experiments.

3.2.2.7 Fundamental Interactions

A. The flux increase would permit increased precision in the neutron decay experiment. In particular, it should be possible to measure the half-life of the neutron with an accuracy better than the present best measurement. This would provide a check of the ratio c_a/c_v in the β-decay interaction.

B. The zero energy n-n scattering amplitude, a measurement of which is of central importance in the understanding of the fundamental nuclear forces, could be measured directly with better precision than will be available in experiments now contemplated.

3.2.2.8 Fast Neutrons

In the fast neutron region, 1 to 100 MeV, new studies of neutron-proton scattering and studies of reactions of the types $(n,x\gamma)$, (n,p), (n,α), (n,d), (n,T), and (n,He^3) could be carried out. Experiments could be initiated which would explore, in minute detail, the differences that may exist in the nuclear forces for neutrons and protons.

3.3 Appendix 3

Comparison of Methods of Neutron Generation

In this appendix, various neutron generating methods are compared first on the basis of continuous production as in a reactor and second on the basis of fast neutron pulse production. We are concerned here mainly with the question of obtaining a high specific source strength (neutrons per cm^3 of source). The question of obtaining a high neutron flux is treated in Appendix 5.

3.3.1 Methods for Continuous Neutron Production

For any neutron generating device the specific source strength is limited principally by the ratio P_R/H_P, where P_R is the power density that can be handled by the cooling system and H_P is the amount of heat deposited in the source per 'useful' neutron escaping from the source.

The principal methods of neutron production that contend as possible high intensity neutron sources are:

(a) Low energy accelerator (e.g. Tandem) using light particle reactions such as $Be^9(d,n)B^{10}$. At 10 MeV bombarding energy, the yield of this reaction is 5.5×10^{-3} n/deuteron[9]. At 15 MeV, it is 1.3×10^{-2} n/deuteron[10].

(b) Electron linear accelerator. Modern electron Linac's used for neutron production deliver pulses of 30 to 150 MeV electrons with peak powers of $\sim$ 100 MW[11]. Neutrons are produced by photo-emission in uranium targets at the rate of about 5×10^{-4} neutrons per electron per MeV[12] at 35 MeV.

(c) Highly enriched, high flux reactor.

(d) Bombardment of heavy elements with protons or other heavy particles of energy between 400 and 1000 MeV from linear accelerators or cyclotrons*.

(e) Fusion devices.

The heat production H_P for these various methods is given, in round numbers, as follows:

	H_P MeV/neutron**
(a) $Be^9(d,n)B^{10}$ 15 MeV	1200
(b) (γ,n) 35 MeV electrons	2000
(c) Reactor†	200
(d) Bi(p,xn) 970 MeV	23 (see Appendix 5)
(e) T + d fusion	3††

* Recent advances in beam conduction in electrostatic accelerators, i.e. control of electron back-flow in the accelerating tube, have removed one of the important limitations to running these devices at very high voltages. However, the problems associated with charging and adequately insulating the terminal are formidable, and, for the present, preclude serious consideration of direct electrostatic methods of achieving high energies.

** Not including the heat taken into the moderator by each neutron.

† Assuming one "useful" neutron per fission, i.e. an escape of one neutron per fission.

†† The fusion neutrons carry a much larger amount of heat ($\sim$14 MeV) into the moderator.

It would appear[13] that the combined problems of containment and high reactivity make it very unlikely that a fusion device will soon produce the large number of neutrons (in a small volume) required for high thermal flux.

Of the remaining methods (d) is clearly to be preferred on the basis of heat production. One of the reasons contributing to low H_P for method (d) is that the loss of energy suffered by the protons in electronic collisions reaches a minimum in the region 600 - 1000 MeV.

We shall next show that the accelerator provides the further advantage of a larger value of P_R compared to that of a reactor. The design of reactor fuel elements is restricted by requirements imposed by criticality. These requirements circumscribe both the materials and geometrical configurations that can be employed. The fuel elements for the various reactors listed in Table I (Appendix 1) are designed for power densities ≤ 4 MW/litre. The same restrictions do not apply to the design of targets for the accelerator. It is estimated that a target 60 cm long by 10 cm diameter consisting of a Pb-Bi eutectic with axial flow velocity of 30 ft/sec and temperature rise of 400°C could be made to dissipate about 36 MW. The corresponding average power density is 8 MW/litre. The maximum power density (at the beam input end of the target) is about 16 MW/litre.

The above considerations of H_P and P_R form the basic physical argument for selecting the proton accelerator for continuous high flux neutron production. An additional factor in favour of the accelerator may be present because of the smaller size of the target (~5 litres) compared to a reactor core (~ 90 litres for HFBR) and the lower absorption in bismuth and lead as compared to the U-Al alloy. This advantage is expressed by the ratio of the thermal flux obtained at a given point in the moderator to the source strength giving rise to that flux. It is shown in Appendix 5 that the ratio of perturbed flux in a beam tube 12 cm from the target to the source strength, for a 60 cm long Bi target in a 120 cm thick D_2O moderator, is

$$\frac{\phi th}{N} = 0.92 \times 10^{-3} \text{ cm}^{-2}$$

For the reactor H.F.B.R. the corresponding ratio at the equivalent position in the moderator with a flux of 7×10^{14} cm^{-2} sec^{-1} and a power of 40 MW[2] is found to be

$$\frac{\phi th}{N} = 0.56 \times 10^{-3} \text{ cm}^{-2}$$

or about one half that for the accelerator.

The neutron production resulting from the bombardment of uranium by deuterons up to 320 MeV has been measured by Crandall and Millburn[14]. It is found that the yield of neutrons per deuteron of energy E is about 25% greater than the yield per proton of the same energy. However, certain disadvantages associated with deuteron acceleration that are not encountered with proton acceleration make a deuteron accelerator unattractive:

(a) The magnetic rigidity of the deuteron is $\sqrt{2}$ times as large as the proton, necessitating higher magnetic field, or larger radius, for the same energy.

(b) Copious neutron backgrounds will be produced at low energy stages of acceleration by stray deuterons striking the walls of the vacuum chamber.

3.3.2 Methods for Pulsed Neutron Production

Inspection of the users' requirements in Appendix 2 shows that the majority of users are either indifferent to, or in favour of, pulsing of the source. All of these are interested in having the average flux exceed 100 times that of NRU, although those doing time-of-flight experiments would presumably still be interested in a facility which realized this increase merely in the peak. It follows therefore that a pulsed source satisfying the majority requirement is one having an average heat production comparable to that of the continuous facility. Therefore, for high fluxes, the conclusions reached for continuous sources in the foregoing section must also apply and, for reasons already given, the high energy proton accelerator method should surpass the electron linac or reactor as a pulsed neutron source.

We note that neutron generators using reactions such as Be^9(dn) or H^3(dn) may give greater intensity than the high energy proton accelerator within selected narrow bands of neutron energy in the MeV range. However, (dn) reactions on light nuclei would not compete with the proton accelerator as a source of pulsed neutrons near thermal energies.

3.4 Appendix 4

Existing High Power Proton Accelerator Design Studies

3.4.1 Comparison of Accelerator Design Parameters

The characteristics of four high current, high energy proton accelerators now under consideration at various laboratories are listed in Table II. These accelerators have been designed primarily for use in high energy physics research and do not necessarily represent the optimum solution for neutron generation. Only two, the proton linear accelerator (P.L.A.) and separated orbit cyclotron (S.O.C.) seem capable of producing the high average beam currents required. Both machines can be run in the continuous wave mode of operation. However, both machines have yet to be proved in the voltage and current range of interest. The highest energy proton linear accelerators in existence today, of which the injector of the Argonne ZGS accelerator is a good example, operated near 50 MeV. The S.O.C. concept is very new although the newness is more a matter of geometrical arrangement than of basic principles. No working models of this accelerator have been constructed up to the present time. Of the two alternatives for neutron generation, the S.O.C. appears to be the most economical both in capital cost and operating cost. The saving in capital cost derives from the more compact size of the S.O.C. and particularly from the more efficient R.F. Cavity System. The latter is also responsible for the saving in operating costs.

3.4.2 The Separated Orbit Cyclotron

The following brief description of the S.O.C. accelerator is condensed from various reports by its inventor, F.M. Russell[19-21].

3.4.2.1 Basic Principles of Design

The equilibrium orbit of the S.O.C. consists of a helical spiral as shown by the solid curve in Fig. 4.1. The ions are guided in the helical orbit by alternating-gradient (strong-focusing) magnets. Placed at intervals of equal azimuthal angle around the helix are radio frequency accelerating gaps represented by the large dots in Fig. 4.1. The gaps lying in any vertical plane belong to a single radio frequency cavity so that the orbit passes through each cavity many times. A constant radio frequency is applied to all cavities and the magnetic field experienced by the equilibrium orbit is adjusted so that an ion which gains energy $eV_o\cos\phi_s$ (V_o is the RF peak voltage and ϕ_s the phase angle) takes exactly one half of an RF cycle, or some multiple thereof, in passing from one gap to the succeeding gap.

With the requirement that the time between successive acceleration is constant (i.e. that the cyclotron frequency

$$f_o = \frac{Be}{2\pi m}$$

is constant and the number of gaps per turn is constant), the radius of curvature of the equilibrium orbit and the strength of

TABLE II

Some Recent High Current Proton Accelerator Design Parameters

Machine	Yale P.L.A.[a]	Los Alamos P.L.A.[b]	Mc^2 Cyclotron[c]	S.O.C.[d]
E_{max} MeV	1000	800	810	1000
Variable Energy	yes	yes	no	yes
Pulse rate pps	28	?	continuous	continuous
Pulse length msec	2	?	"	"
Duty cycle %	5.6	6	100	100
Peak beam current ma	50	17	0.1	1
Avg. beam current ma	2.7	1	0.1	1
Peak beam power MW	50	14	0.08	1
Avg. beam power MW	2.7	0.8	0.08	1
Extraction efficiency %	100	100	80	100
Cavity losses MW	86	(~60)	-	13
Machine cost[e] $	30M	25M	~10M	{16M 9M

(a) See refs. 15 and 16
(b) See ref. 17
(c) See refs. 7 and 18
(d) See refs. 19-21
(e) Exclusive of site, buildings and research equipment

UNCLASSIFIED
ORNL-LR-DWG 74595R

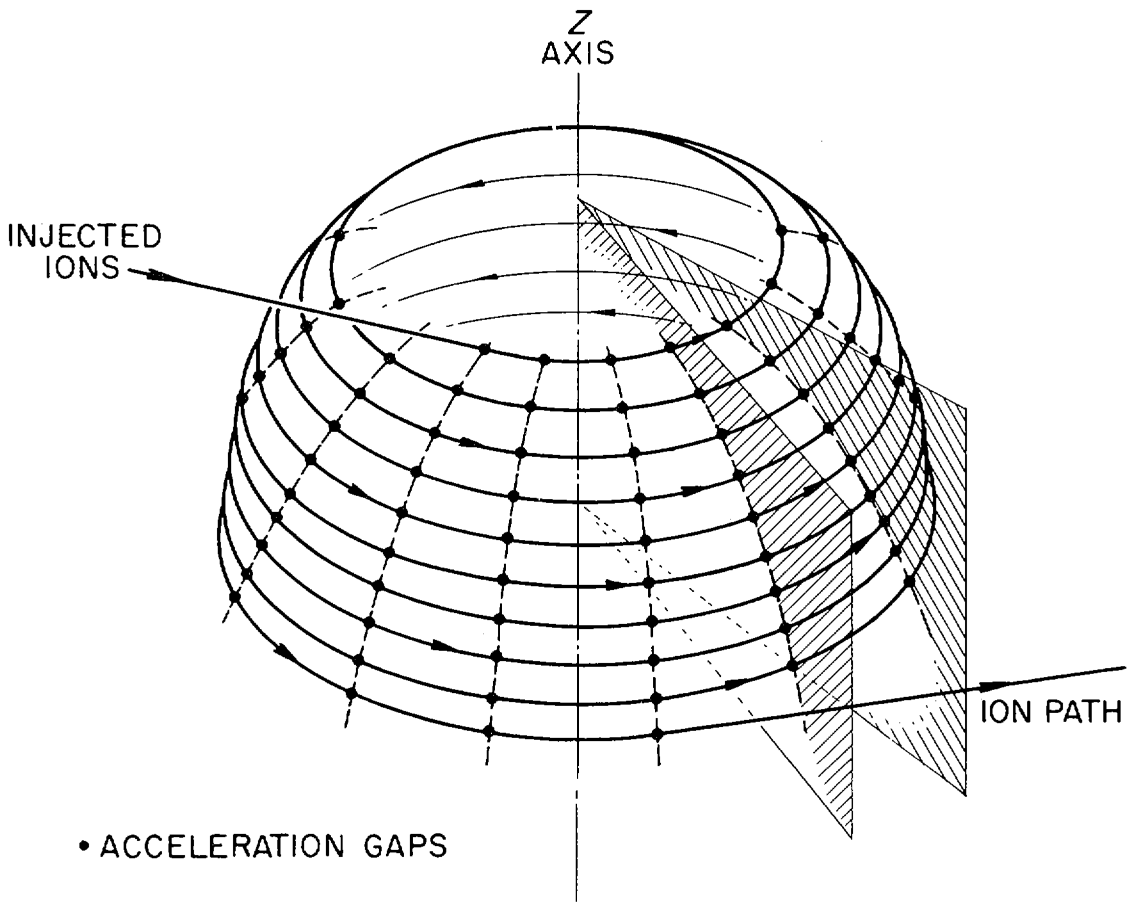

Fig. 4.1 Diagram of beam path with both radial and axial separation. Accelerating gaps are indicated by dots along the beam path. The rf voltages at the gaps joined by dashed line are in phase.

the magnetic field at the a'th accelerating gap are functions of the ion energy only, apart from a scale factor. The radius of curvature is given by

$$r_a = (1-1/\gamma_a^2)^{1/2} r_o$$

where γ_a is the ratio of total energy of the ion at the a'th gap to the rest mass energy and r_o is the cyclotron unit

$$r_o = c/(2\pi f_o)$$

The field strength at the a'th gap is

$$B_a = \gamma_a B_o$$

where B_o is the field at zero energy. The parameters B_o and r_o are related by the expression

$$B_o = m_o c/(e\ r_o)$$

These parameters govern the size of the accelerator and must be compatable with a number of additional requirements among which are the following:-

(a) The separation between R.F. cavities must be large enough to accommodate strong-focusing magnets capable of stabilizing the orbit in the field B_a. The region of stability is a function of the number of gaps per turn, the length of a 'cell' (magnet plus gap) and the strength and gradient of the field.

(b) The space available for accelerating gaps and the number of gaps per turn must be compatible with a practical R.F. cavity design. The cavity must be of simple construction and must operate in the required resonant mode. It must also have low losses and be free of voltage break down for the accelerating voltages required.

(c) The dimensions of magnets and R.F. cavities must be such that machining and 'line-up' tolerances can be easily met.

(d) The cost of the accelerator should be kept to a minimum. The cost is a function of the size of the magnets, the number of cavities, and the size of the power supplies for both magnets and cavities.

3.4.2.2 Design Details

A sketch of a radio frequency cavity system suggested by Russell[19] is shown in Fig. 4.2. This cavity which is suitable for operation in the transverse-electric (TE) mode can be built with a satisfactorily high unloaded Q of about 2×10^4. Further details are given in ref. 21. A sketch of the geometrical arrangement of cavities strong-focusing magnets, and beam tubes is shown in Fig. 4.3.

Because of the shorter distance covered by the ion per R.F. period at low energies, it is not possible at the low energy end of the spiral to find room for the same number of cells that are conveniently fitted in per revolution at the high energy end. In the design outlined by Russell[19] this difficulty is overcome by using a linear accelerator to cover the lowest energies (0 to 15 MeV) while the range above 15 MeV is divided into two stages of

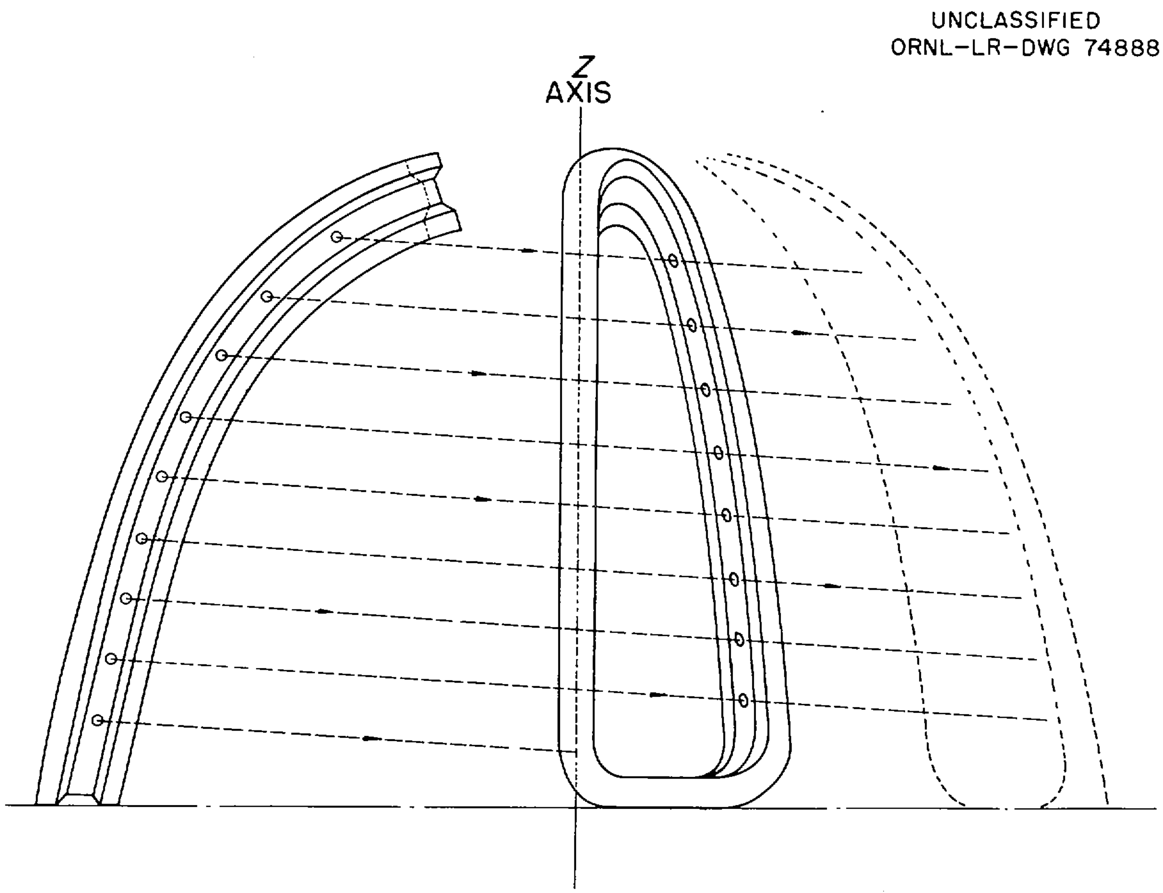

Fig. 4.2 Sketch of part of suggested radio-frequency cavity system. The electric field is a maximum at the center of the cavity and is parallel to the path of the ions. The separation along the equilibrium orbit between two sets of gaps is simply $\beta\lambda/2$ where λ is given by $2\pi mc/NeB_o$ and N is the number of such cavities.

UNCLASSIFIED
ORNL-LR-DWG 76872

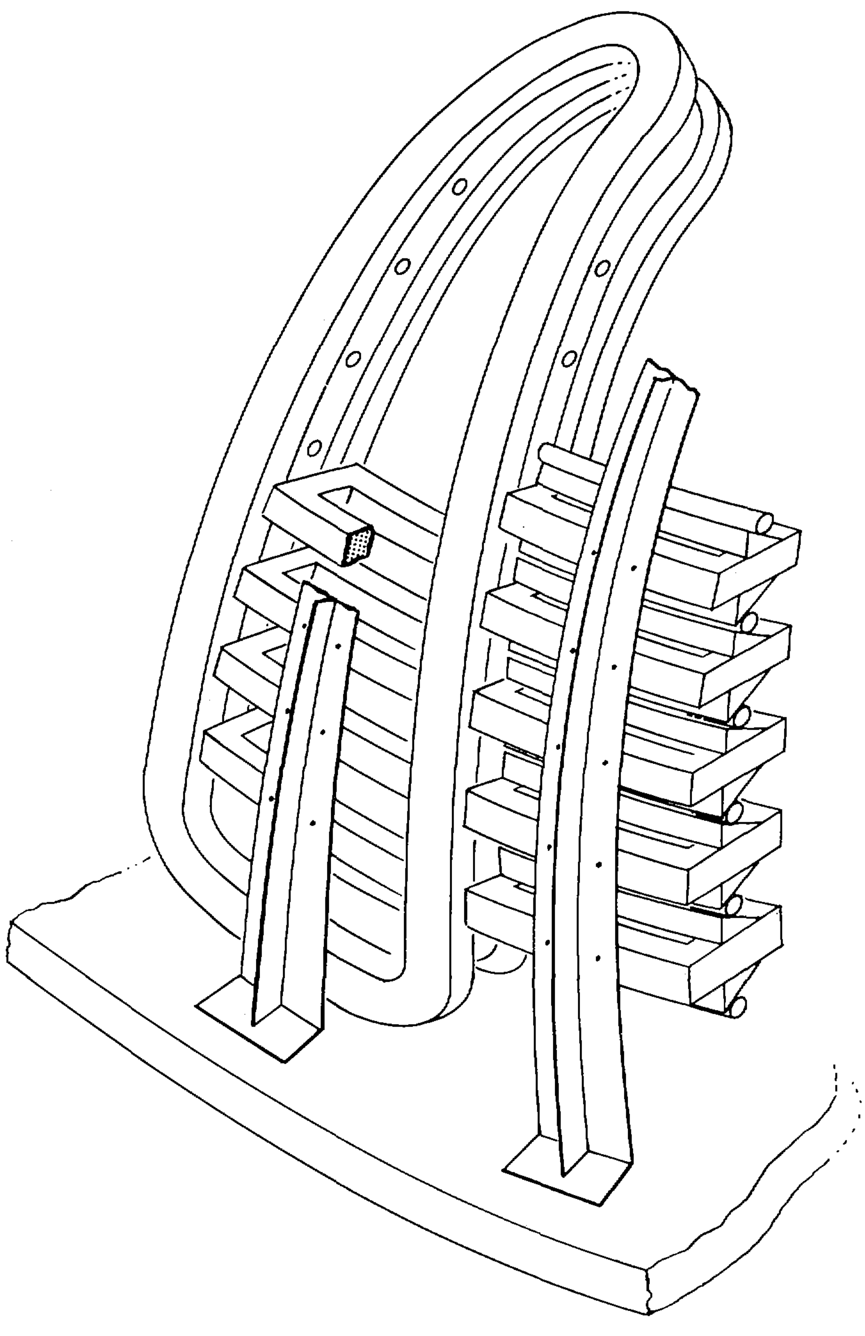

Fig. 4.3 Sketch of a complete magnet and rf cavity sector. Each sector contains one rf cavity and pairs of magnet cells, the positive and negative gradient sections being mounted upon a common support so that the magnet pairs can be aligned accurately.

UNCLASSIFIED
ORNL-LR-DWG 76891

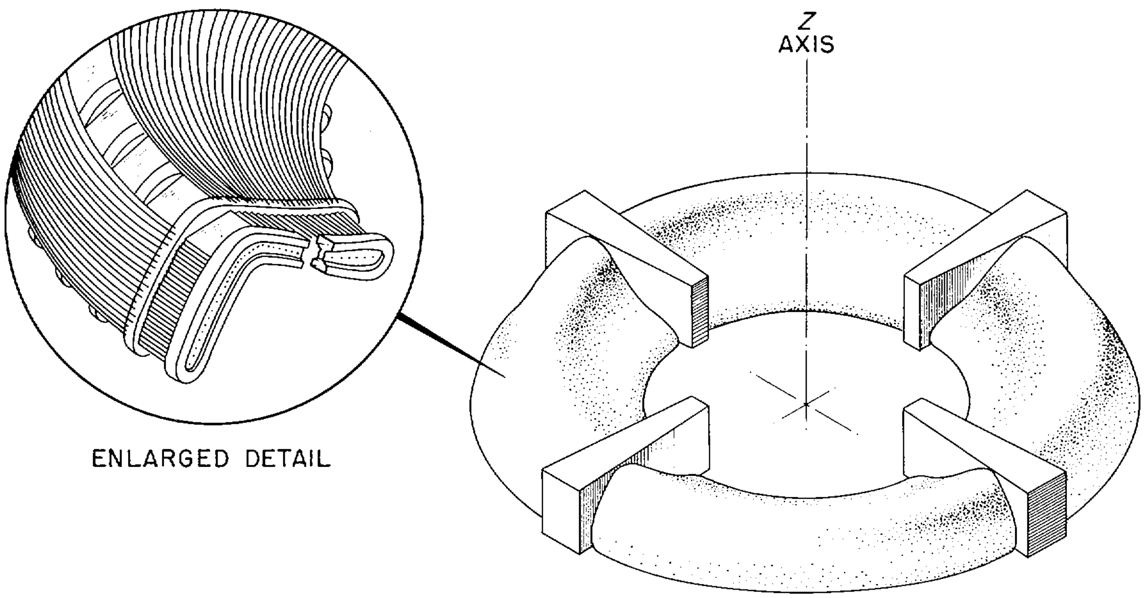

Fig. 4.4 Artist's sketch of whole machine showing location of wedge sections and the folded nature of the machine. The insert shows details of the rf cavities, the coils, and the arrangement of the magnet stacks.

UNCLASSIFIED
ORNL-LR-DWG 76886

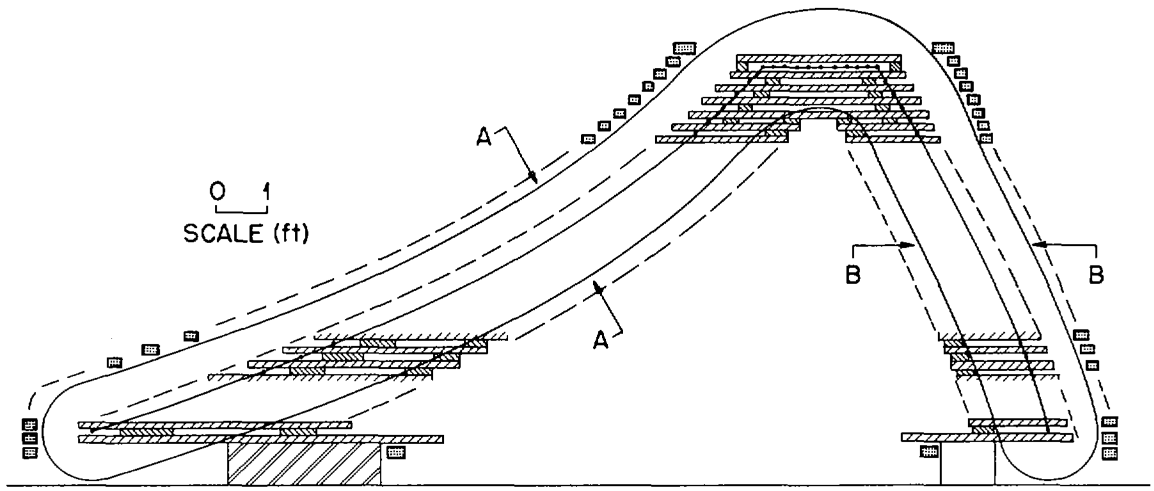

Fig. 4.5 Radial-cross section of an SOC intended to accelerate protons from 120 MeV up to 1 GeV. A single rf cavity is used and is bent at the mid-energy point. End coils for correcting the magnetic field distribution are indicated at both top and bottom of the coil system. The successive points tranversed by the beam are indicated by dots.

SOC acceleration, 15 to 120 MeV, and 120 MeV to the final energy. The cyclotron frequency and R.F. frequency of the higher energy stage is maintained in the lower but the number of accelerations per RF cycle is reduced from two to one and hence the spacing between accelerating gaps is increased by a factor of two allowing more room for magnets and cavities.

An alternative to the beehive configuration of Fig. 4.1 is shown in Fig. 4.4. Here the direction of progression of the turns in the z-direction is reversed near the mid point giving a much more compact and rigid structure with a resulting saving of magnet iron. A radial section through this accelerator is shown in Fig. 4.5. Straight sections are provided in the beam tubes in each quadrant to provide necessary space for magnets imparting the z-motion and for injector and extractor magnets.

3.4.2.3 Design Parameters

A partial list of parameters extracted from the design outlined by Russell[19] are given in Table III. These quantities are intended only to show the scale of the accelerator and do not represent a complete or final specification.

A summary of costs estimated by Russell is given in Table IV. In prepartion of these estimates, the following assumptions were made:

1. Output - proton beam current 1 ma, mean, at 1 BeV
2. $\phi_s = 20^\circ$
3. DC to RF conversion efficiency 60%
4. RF power supply at $165/kw of delivered RF.

5. Tubes, 500 kw, at $100/kw
6. Cavities at $\$20/ft^2$
7. Coils at $3/lb
8. Magnet poles and blocks at $0.50/lb
9. Pole shims $40/ft of ion path first stage and $20/ft second stage
10. R.F. circuits etc. $130/kw.

3.4.2.4 Discussion of the S.O.C. Concept

The following desirable features of the S.O.C. have been noted:

1. Because the beam passes each point in the machine only once, many resonances encountered in other types of cyclic accelerator are avoided. In the ideal case only the basic instabilities common to all alternating gradient systems exist and these present no difficulties in design[19]. However, the permissable tolerances on position of magnets and field gradients are of importance. Preliminary estimates indicate that tolerances on mechanical adjustment of guide magnets about the equilibrim orbit could be $\pm 5 \times 10^{-3}$ in. The corresponding field error is 1 in 10^3 which is a moderately relaxed tolerance for a fixed field device[19]. The tolerance on the regulation of R.F. voltage amplitude appears to be no more stringent than for a linear accelerator.

2. Both the amount of R.F. cavity per acceleration and the field strength is less than that required for a proton linear accelerator. The cavity losses are 13 MW for the S.O.C. compared to about 60 MW for a P.L.A. at 1000 MeV (see Table II).

3. The size of building required to house an S.O.C. is much smaller than that for a P.L.A.

Table III

Accelerator Parameters For 15-1000 MeV SOC[19]

f_o, cyclotron frequency (Mc/s)		3.82
r_o, cyclotron unit (in)		555
f_r, frequency in cavities (Mc/s)		191
B_o (kG)		2.25
Number of gaps in 60 turns (2nd stage)		6000
Electric field strength in cavity (kV/in)		37
Total Power loss to cavities, both stages $\phi_s=20^\circ$(MW)		10.1
Beam loading at 10 mA mean, both stages (MW)		9.8
Magnet height, 2nd stage (ft)		7.5
	at 120 Mev	at 1000 MeV
Magnet radius 2nd stage (ft)	21.5	40
B 2nd stage (kG)	4.50	4.88
Weight of magnet iron, less shims, both stages(tons)		650
Weight of copper, both stages (tons)		384
Total magnet power, both stages (MW)		2.88

Table IV

Accelerator Cost Estimate[19]

		$M
Cockcroft-Walton Injector		0.250
15 MeV Linac		1.480
First Stage SOC		
Magnets and Power Supply	0.970	
Cavities and RF Parts	.400	
RF Power Supply and Tubes	.450	
Vacuum System	.100	
		1.920
Second Stage SOC		
Magnets and Power Supply	3.882	
Cavities and RF Parts	2.330	
RF Power Supply and Tubes	2.250	
Vacuum System	.100	
		8.562
Miscellaneous		.750
		12.962
Contingency 20%		2.59
Total		15.55

Among disadvantages of the S.O.C. machine are the following:

1. Construction of the S.O.C. may be more expensive than noted by Russell because of the uniqueness of each piece. For example in the first stage some 1100 magnets are required, each with a different radius of curvature, length and field strength. It may be possible to economize by using a standard magnet design with special pole faces for each magnet as required, but construction may still present more problems than for more conventional accelerators.

2. An approximate calculation of phase defocusing caused by space charge effects indicates that a limit of average beam current may be encountered near 100 ma. This limit is not much greater than the required current (see section 1.4) and suggests that a full scale investigation of this aspect of the machine is desirable.

3. The S.O.C. is a variable-energy machine only in so far as it is possible to extract the beam at various stages along the spiral. The changing of beam energies therefore involves shifting the extraction magnet from one position to another with attendant cumbersome modifications in the beam transport system.

4. The designs for the S.O.C. described in Russell's study[19] are very preliminary and are intended only to establish the feasibility of the separated orbit principle. Many improvements would no doubt come to light in a serious design study. It is noted

that the division of the accelerator into two separate stages as in Fig. 2 is somewhat arbitrary. While a change in mode of operation may be necessary near 120 MeV, there is much latitude in geometrical arrangement of the two stages; for example, they could be mounted one on top of the other or the beehive structures could be inverted if there was a structural or economic advantage to be gained in doing so.

3.5 Appendix 5

Parameter Optimization for Continuous Neutron Production

In this appendix consideration is given to the optimum choice of target, moderator, beam energy and beam current to produce at minimum cost the required flux of 10^{16} n cm^{-2} sec^{-1}. Because of many uncertainties as yet unresolved concerning neutron yields as a function of neutron energy and target geometry, no more than a rough determination of the optimum operating conditions is justified.

3.5.1 Target

The selection of the optimum target material for the production of neutrons by the (p,xn) reaction depends on the neutron yield per proton and the heat accompanying each neutron[22], H_p (appendix 3). Although, as shown experimentally by Bercovitch, Carmichael, Hanna and Hincks[23], the neutron yield increases with mass number, materials such as U^{238} and Th^{232} must be ruled out as targets because in these materials a significant increase in H_p occurs due to fission processes following the proton interaction. If, for example, only one fission event occurred per proton interaction in U^{238} (an underestimate for a thick target), H_p would be about 30 MeV per neutron at a bombarding energy of 1 BeV as compared to 23 MeV in the absence of fission. Therefore, in the present application where the object is to produce a large neutron flux, the necessity of minimizing the heat produced in the target imposes a lower limit with a uranium target than with a material such as bismuth for which the fission contribution is negligible. A further argument against the use of uranium is its relatively high absorption of thermal neutrons. A promising target material with excellent heat transfer possibilities would appear to be a Pb-Bi eutectic . On the other hand where a large neutron production, but not necessarily large flux, is required, the use of a uranium target is indicated[6].

The optimum target dimensions can only be determined by a detailed study of the dynamics of the cascade and evaporation processes occurring in the (p,xn) reaction. A Monte Carlo calculation designed to answer these questions is in progress[22]. Consideration of the effective nuclear interaction length (20 cm) for high energy protons in bismuth, with rough estimates of the beam spread during the cascade and target cooling requirements, have lead to the adoption, in the present analysis, of a target of length 60 cm and radius 5 cm as shown in Fig. 1.

3.5.2 Moderator

The thermal neutron flux at the source end of a beam tube for a target of given dimensions depends on the dimensions and material of the moderator, the thickness of the moderator between the target and the tube and the dimensions and materials of the tube. From considerations presented in appendix 9 , it is concluded that a cylindrical D_2O blanket of thickness 120 cm and length 300 cm (Fig. 1) would be desirable. The cost of D_2O in the complete system, including heat exchangers, etc would be about \$1M at \$20/lb. In a refined design, involving considerations of such diversematters as the detailed shape of the target assembly and the optimum number and placement of beam tubes, it may be possible to arrive at a more nearly spherical moderator shape with considerable economy of the D_2O inventory.

The thickness of D_2O between target and beam tube adopted in the present analysis is similar to that used in the HFBR reactor[2], viz. 12 cm. The flux depression caused by the presence of 8 beam tubes around the HFBR core is 30%. The flux depression for the present arrangement assuming the same number of tubes has been estimated with certain simplifying assumptions for beam tube geometry to be a factor of 2.

3.5.3 Determination of Neutron Source Strength

By scaling from Figs. 10.5, 10.7 and 10.8, appendix 10, we estimate the mid plane flux at the end of a beam hole to be

$$\phi_{th} = 0.92 \times 10^{-3} \text{ N cm}^{-2} \text{ sec}^{-1}$$

where N is the source strength and where it is assumed that the neutron production is uniform along the 60 cm length of the target. The design flux value of 10^{16} n cm^{-2} sec^{-1} would therefore be obtained with a source strength

$$N = 9 \times 10^{18} \text{ sec}^{-1} \quad .$$

3.5.4 Cost Optimization

3.5.4.1 Basic Considerations

It is reasonable to assume as a first approximation that the cost, C, of a high energy proton accelerator will contain contributions proportional to the energy E and to the beam power, i.e.,

$$C = aE + bP = E(a+bI)$$

where I is the beam current. C may be made the capital cost, the operating cost, or any suitable combination of the two by suitable choice of a and b. For the present required source strength of 9×10^{18} n sec^{-1}, we may write

$$I = 1.5 \times 10^3/\nu(E) \qquad \text{ma},$$

where $\nu(E)$ is the number of neutrons produced in the target per proton of energy E. Thus if the functional form of $\nu(E)$ is known, it is possible to determine the energy E and current I at minimum cost, for values of a and b dictated by the economics of the accelerator.

There are no direct measurements of the thick target yield, $\nu(E)$, in bismuth. The cascade and evaporation neutron yields derived for uranium by Russell[24] from measurements of Meadows, Ringo and Smith[25], when transformed to bismuth using a mass dependence obtained from Bercovitch et al.[23] are about a factor of 3 higher than the yields quoted by Wallace and Sondhaus[26] for lead. Their values are apparently based on Fig. 1 of Moyer[27]. Recent Monte Carlo calculations[23] performed at Chalk River suggest values about 3/5 of the Russell-Smith values in the range of proton energies 0.3 to 1 BeV. These calculations depend strongly on the intra-nuclear cascade calculation of Metropolis et al.[28,29] and the evaporation calculations of Dostrovsky, Rabinowitz and Bivins[30]. When these calculations are compared with experiment, the agreement is usually satisfactory for the average number and energy of particles, though poor for a specific reaction, for instance the (p,2n) reaction. The principal uncertainty of the present calculation probably arises from the normalization to the neutron yields per interaction obtained by Bercovitch et al[23]. The internal consistency of their measurements would indicate an uncertainty of about ± 20%. However, for 500 MeV protons on uranium, the yields obtained by Crandall and Millburn[14] are about 40% higher than Bercovitch et al., and those of Meadows, Ringo and Smith[25] about 50% lower. Bearing in mind these uncertainties, the provisional results of the present calculations can be fitted in the range 0.3 to 1 BeV by the linear relation

$$\nu(E) \approx -4.57 + 28.6\,E \quad \pm \; 50\% \qquad (E \text{ in BeV})$$

for a metallic bismuth target 5 cm in radius, 60 cm long.

3.5.4.2 Cost Optimization and Parameters for S.O.C.

From cost information given by Russell[19] (appendix 4) we may evaluate parameters a and b and hence, on the basis of the above relations, determine the minimum cost solution for both capital and operating costs. For the purposes of the present optimization calculation, capital costs include RF power equipment, magnets, coils, vacuum chamber, cavities and injector but not D_2O, buildings, or research equipment. The latter items will be included in the cost summary, section 3.5.4.3. Similarly, the operating cost used in the calculation is the cost of power only, which was assumed to be delivered at $35/kW year. Other operating costs such as power tube replacements, salaries, and research expenses are given in section 3.5.4.3. Parameters obtained on this basis are given in Table V.

Table V Parameter Optimization

Item	Capital Minimum	Operating Minimum
a	12.3×10^6 $/BeV	0.45×10^6 $/BeV year
b	0.39×10^6 $/MW	0.035×10^6 $/MW year
E(MeV)	732	970
I(ma)	92	65
Beam Power (MW)	67	63
Cavity Power (MW)	9.6	13
Total R.F. (MW)	77	76
Magnet Power (MW)	2.3	3.0
Target Heat* (MW)	43	35
Capital Cost ($M)	39.4	42.1
Annual Power Cost ($M)	4.55	4.51

* From the Monte Carlo calculation[22]. A small contribution (about 5%) from the small number of fissions occurring in the bismuth is included, but not the contribution from β-decay, for which see section 3.5.4.4.

The two solutions are close together in cost and in view of the very approximate nature of the neutron yield information there is little justification on economic grounds for choosing one over the other. For the same reason the absolute values of the parameters in either solution should not be taken very seriously. In this report, the operating minimum solution is chosen because it calls for the higher energy and lower current. These operating conditions are the more attractive for several reasons:

(a) High currents are more difficult to produce (ion source problems) and to handle (space charge repulsion) than low currents. No such technical difficulties are associated with higher energies.

(b) With constant beam power and beam area the heat released per unit volume of the target is less for high energy and low current than for low energy and high current.

(c) Both the kinds of mesons produced and the intensities of the meson beams increase with increasing energy (see appendix 8).

Moreover, the costs increase rather slowly with E above the minimum and considerations such as the three just mentioned may ultimately justify a decision to operate at even higher energies.

3.5.4.3 Summary of Costs for S.O.C.

3.5.4.3.1 Capital Costs

No detailed study of costs other than those for the accelerator itself has been made. In the following we give order of magnitude estimates using as a guide estimates for the Yale P.L.A.[15] where local estimates are not available.

1.	D_2O (section 3.5.2)		\$ 1.0M
2.	Electrical feed equipment, i.e. substation		0.5
3.	Building		
	Accelerator room, area 10^4 sq. ft. = 10% of Yale P.L.A. area, i.e. 0.1 x \$3.4M =	\$0.3M	
	Experimental and service areas, including beam handling and special shielding (estimate)	4.0M	
	Target assembly (estimate)	4.0M	
			8.3
4.	Research equipment estimate		2.0
			11.8
	970 MeV accelerator (section 3.5.4.2)		42.1
	20% contingency		10.8
	Total Capital cost excluding engineering design costs		\$64.7M

3.5.4.3.2 Annual Operating Costs

Again the estimate for the Yale P.L.A. is used as a guide.

Salaries and overhead	\$1.0M
Research operations	1.0
Tube replacement (less than for P.L.A.)	0.5
Other utilities, supplies, services etc.	0.2
Power with E_{rf} = 60% at \$35/KW year	4.5
Total annual operating cost	\$7.2M

3.5.4.3.3 Comparison of Costs of S.O.C. and High Flux Reactor

It is of interest to compare the capital and operating costs of the accelerator as a neutron source with those of a high flux reactor operated in Canada. The reactor will be assumed to be similar to H.F.B.R. with a flux of 7×10^{14} cm^{-2} sec^{-1} and source strength of about 1.2×10^{18} sec^{-1} (the value calculated assuming a power of 40 Mw and H_p = 200 MeV per neutron). The capital cost is taken to be \$12M, which is approximately the value quoted for H.F.B.R.[31] The reactor operating cost is crudely estimated using as a guide the costs of enriched fuel for the NRU reactor and the operating costs of the NRX and NRU reactors, excluding costs of engineering experiments, Co^{60} production facilities, and other reactor facilities of research nature. The operating cost so obtained is \$1.5 ± 0.2M per annum. For the S.O.C., an annual operating cost (exclusive of research expenses) of \$6.2M is assumed.

	S.O.C. \$M	Reactor \$M
Capital cost per unit 10^{14} cm^{-2} sec^{-1} flux	0.65	1.7
Capital cost per unit 10^{18} sec^{-1} source strength	7.2	10
Annual operating cost per unit 10^{14} cm^{-2} sec^{-1} flux	0.062	0.22
Operating cost per gram of neutrons	0.013	0.029

It is evident that the accelerator represents a substantial improvement over the reactor in the unit costs for neutron production. The differential would be still greater for reactors designed to give fluxes approaching 10^{16} cm^{-2} sec^{-1}.

3.5.4.4 Target Heating

The neutron yield at 970 MeV is 23.4 neutrons/proton[22]. Neglecting inelastic scattering in the target, each neutron carries out ~ 17 MeV, a net energy of ~ 23 MeV/neutron or ~ 540 MeV/proton being left in the target. For a current of 65 ma, the heat dissipated in the target is then 0.54 x 65 = 35.1 MW.

The heat generated by radioactive decay in the Bi target is small. This effect, which is in contrast to that obtaining in a reactor fuel element, arises from the fact that the valley of stability tends to run parallel to Z = 82 for decreasing A. On the average, a 970 MeV incident proton will cause spallation in 2 or 3 nuclei. Most of these will have emitted at least one proton. Thus the products in a bismuth target will be mainly neutron deficient lead and thallium isotopes with fewer neutron deficient bismuth isotopes. The average β^+ decay energy (including annihilation radiation) of this group of nuclides will be less than $\sim$ 5 MeV/proton, i.e. less than $\sim$ 0.5 MW will be deposited in the target.

The heat generated by neutron capture in bismuth and the subsequent radioactive decay of Bi^{210} and Po^{210} is also small compared to the heat deposited by the proton beam. In a flux of 10^{16} cm^{-2} sec^{-1} there will occur about 10^{12} RaE and Po^{210} decays/sec/gm of bismuth at equilibrium. The average decay energy is $\sim$ 5.88 MeV or $\sim$ 1 watt/gm. For a 50 kgm target this results in a total heat production of 0.05 MW.

The total heat generated in the target 60 cm long and 10 cm diameter is in round numbers, 36 MW. It is estimated that this heat can be dissipated by axial flow of a Pb-Bi eutectic at 30 feet per second with a 400°C temperature rise.

3.6 Appendix 6

Provision For Pulsing

3.6.1 Pulsing of Proton Beam

3.6.1.1 Introduction

The proton beam in devices using radio frequency acceleration is necessarily 'bunched' into distinct packets which arrive at each succeeding RF gap within a limited range of the phase angle, ϕ_s. Particles arriving outside this phase acceptance region are lost to the walls of the accelerating tube. In the S.O.C. the phase acceptance (duty cycle) is typically 16%[19]. Therefore, at 200 Mc/s cavity frequency, the S.O.C. beam exhibits a 'microstructure' of 0.8 nsec pulses spaced 5 nsec apart.

It has been suggested[15] that beam microstructure may be of value for certain fast time of flight applications. It may be convenient in some experiments to use these pulses at the full 200 Mc/s repetition rate, but it seems likely that arrangements whereby only occasional packets, e.g. 1 in 100, are deflected to a separate target would be found more useful. In the latter case, such experiments could be carried out simultaneously with others experiments making use of the remaining 99% of the beam at a second target location.

For many experiments it is desirable to use proton pulses of duration long compared to the R.F. period. The production of these 'macroscopic' pulses can be effected either initially, by pulsing the ion source and accelerating the pulsed beam or by accelerating a continuous beam and providing some means of creating pulses (bunching) after acceleration. One principal disadvantage of the first method is that the instantaneous currents in the pulses are very large and lead to space charge effects in the accelerating system at low energies. A second disadvantage is that the R.F. power in the accelerating cavities must either be left on between pulses, which is wasteful of power or must be switched off and on between pulses. In the latter case, the necessary radio-frequency and modulating equipment appears to be several times more costly per unit of average beam power than for c.w. operation. Furthermore, the buildup time of the R.F. power in the pulse limits the pulse structure that can be accelerated efficiently to pulses longer than about 50 microseconds. A final disadvantage of pre-acceleration pulsing is that it removes the possibility of obtaining a continuous neutron source, except perhaps for thermal neutrons, where the long die-away time in a thick D_2O moderator could act to smooth out the pulse structure. Clearly for the present application it is desirable to have continuous acceleration and a facility for post-acceleration bunching.

Whether the S.O.C. proton beam is extracted in the continuous wave mode of operation or whether it has been subjected to post-acceleration macroscopic bunching, it will probably retain the RF microstructure. Techniques for 'debunching' or smoothing this fine structure have been described[32,33]. Debunching may be necessary for certain experiments which cannot tolerate high instantaneous counting rates.

3.6.1.2 Proton Storage Ring

A proton storage ring arrangement is shown schematically in Fig. 2. The 970 MeV proton beam from the S.O.C. is guided into a magnetic ring structure where it is continuously 'stacked' in an orbit for a pre-determined length of time. Subsequently, the stacked beam is ejected from the ring into the target in a time short compared to the storage time. Ideally it would be desirable to produce pulses of about 10^{-7} sec duration with a repetition rate of about 200 sec^{-1}; if the whole of the continuous beam were to be converted to pulses the storage time would necessarily be 5 milliseconds.

Up to the present time, no proton storage rings have been put in operation with high energy accelerators. Storage rings for electrons have been devised and proven to be successful[34,35]. Partly as a result of this success and partly because of growing interest in colliding beam experiments with high energy protons of 25 to 300 BeV, the feasibility of proton storage rings has been discussed recently in much detail[36-38]. However, in the present application at lower energies, the storage capacity of such rings is reduced and it would appear not to be feasible to stack the entire S.O.C. output for 5 milliseconds without considerable modification in design. No detailed investigation of optimum storage methods has been attempted in the present study. For purposes of comparison with other pulsing methods, we shall assume below that a practicable method can be devised for converting the entire continuous beam to 10^{-7} sec-long pulses at 200 pps.

Among conditions determining the number of protons that may be stored in a ring and the length of storage time are the following[36,37,39,40].-

(a) Vacuum:

The vacuum in the storage ring must be sufficiently low that the circulating beam is not appreciably attenuated during the storage time. That this is readily attained has already been demonstrated in the CERN Accelerator where 9-10 BeV circulating proton beams have a maximum life of 2 minutes at 2×10^{-6} mm Hg[41].

(b) Phase Space Considerations:

A theorem in dynamics (see ref. 42 under Liouville) states that the volume in phase space occupied by a group of particles is a constant of the motion. Since any practical storage ring can contain particles in only a finite region of phase space, the number of particles which the ring can hold is limited. Courant[36] has estimated this limit for a storage ring at 300 BeV with certain assumptions about the dimensions and momentum spread of the beam at injection and about the range of momentum over which a proton can be held in the ring. When the calculation is adapted to protons of energy $\sim$ 970 MeV, it is found that a storage ring can contain only about 150 turns of particles. For a 5 millisecond storage time in an 80 ft dia. ring, 1.5×10^4 turns must to stacked. Thus a method of increasing the storage capacity by increasing the range of momentum over which storage is possible in any one ring, by using multiple rings placed side by side with their planes normal to the same magnetic field, or by some other method would appear to be necessary if the entire output of the S.O.C. is to be converted to pulses at 200 pps.

(c) Space Charge Limitations:

Transverse de-focusing may occur in the ring because of space charge. This difficulty has been discussed by Courant[36] who believed that it could probably be overcome in the high energy storage ring he was considering. Even assuming it were possible to store the whole beam, it would appear that the charge density in our case would be made less than Courant's. Therefore, space charge limitations are not obviously prohibitive.

Mutual coulomb scattering by the particles in the beam is important in electron storage rings. However, application of the theory of this effect[43] to storage of the full 970 MeV proton beam for a storage period of 5 milliseconds shows that the scattering effect would be negligible.

Extraction of the stored beam from the ring also presents formidable problems in design. Practicable methods probably would involve ejector magnets[35,44] which can be pulsed on for intervals as short as 10^{-5} sec with rise times of 2 x 10^{-7} sec. A vital consideration is to prevent even a small fraction of the beam from striking the walls of the vacuum chamber where it will give rise to secondary radiation, induced activities, and local heating which in severe cases could have catastrophic consequences.

3.6.2 Neutron Pulsing

As discussed in appendix 2, various experiments requiring pulsing have been proposed over the whole range of neutron energies. Fast neutron experiments in the energy range 1 to 100 MeV require short pulses $< 10^{-8}$ seconds. For such experiments deflection of occasional individual microstructure pulses to a suitable target would produce an ideal neutron source. If it were desirable to extract the proton pulses after about 100 MeV of acceleration, such a facility might conveniently be placed between the first and second stage of the S.O.C. at 120 MeV. As mentioned earlier, this facility could be operated without appreciable loss of beam to other users. It must also be operated in such a way that no appreciable portion of the beam is scattered to the walls during the pulse extraction process.

Resonance neutron time of flight experiments typically require pulses of length less than 10^{-6} sec. Such pulses may be produced by bombarding a thin target, thin moderator assembly with 970 MeV protons using selected microstructure pulses, or the $\sim 10^{-7}$ sec-long pulses produced by a storage ring. The extraction of individual microstructure pulses will be more difficult at 970 MeV than at 100 MeV; no study has been made of possible ways this may be done.

Thermal and epithermal time of flight experiments require pulses in the range 10^{-5} to 10^{-6} sec approximately. Such pulses could be produced by bombarding a thick target with protons from a storage ring, the target being surrounded by a moderator of optimum thickness to give pulses of the energy required. For good resolution a chopper must be used in synchronism with the pulses from the accelerator (see section 3.6.2.2).

3.6.2.1 Resonance and Fast Neutron Intensities

The neutron intensities and pulse lengths obtained from resonance and fast neutron target assemblies depend strongly on the geometry and other properties of the target and moderator. The problem of choosing optimum moderator conditions, has been discussed in detail by Michaudon[45].

In this section we shall compare various pulsed neutron devices as fast neutron sources divorced from the moderator question which applies equally to all such devices. A rough figure of merit for comparing different pulsed neutron source for time-of-flight work is:

$$M = \frac{J_a}{T^2} = \frac{J_p \times f}{T}$$

where J_a and J_p are respectively the average and peak <u>unmoderated</u>

4π neutron outputs in the shortest pulses of which the source is capable in neutrons per sec, f is the repetition rate in sec^{-1}, and T is the pulse length in seconds. It is assumed that the sources compared give the same neutron energy spectrum, that there are no restrictions on the flight paths, and that all parts of the source are effective in producing fast neutrons. The pulse length enters as the square because, to maintain time resolution, changes in T must be compensated by changes in flight path which affect the counting rate through the inverse square law.*

Figures of merit for various time-of-flight facilities are compared in Table VI. For purposes of comparison it is assumed that the present accelerator can be operated in three modes:

1. Continuous bombardment of a thick target; pulses produced by a chopper with characteristics identical to those of the fast neutron chopper at N.R.U.

2. Storage ring pulsing with a thin target stopping only 1% of the proton beam. It is assumed that the full output of the accelerator can be converted to pulses by the storage ring.

3. Microstructure pulses of 970 MeV protons deflected at rate of 1:100 to a thin target stopping 1% of the beam.

On the basis of this figure of merit it would appear that the present accelerator, in either of modes 2 or 3, is superior by several orders of magnitude to other time-of-flight sources

* Assuming the target area is smaller than that of the beam.

Table VI

Figure of Merit For Fast Neutron Time-of-Flight Facilities

P_p and P_A are peak and average power delivered to target. All other symbols are defined in the text.

Facility	J_P sec^{-1}	J_A sec^{-1}	P_P MW	P_A MW	f sec^{-1}	T sec	M sec^{-3}	Ref.
Rensselaer electron Linac[a]	$4x10^{17}$	$2.6x10^{12}$	130	$8.4x10^{-4}$	720	$9x10^{-9}$	$3.2x10^{28}$	11
Nevis Cyclotron	10^{19}	$1.2x10^{13}$			60	$2x10^{-8}$	$3x10^{28}$	46
Pulsed Reactor I.B.R.[b]	$\sim 10^{17}$	$3x10^{13}$	3	.01	83	$3.6x10^{-7}$	$2.4x10^{18}$	47
N.R.U. Fast Neutron Chopper[b,c]	$1.4x10^{16}$	$1.5x10^{13}$	-	-	$1.3x10^{3}$	$8x10^{-7}$	$2.3x10^{25}$	
Present accelerator, chopper[d]	$1.8x10^{19}$	$1.9x10^{16}$	-	-	$1.3x10^{3}$	$8x10^{-7}$	$3x10^{28}$	App.5
Present accelerator, storage ring[e]	$1.5x10^{21}$	$9x10^{16}$	$8x10^{3}$	0.47	200	$3x10^{-7}$	$1x10^{30}$	App.5,6
Present accelerator,Microstructure[f]	$5.7x10^{17}$	$9x10^{14}$	3	$4.7x10^{-3}$	$2x10^{4}$	$8x10^{-10}$	$1.4x10^{35}$	App.5,6

a - Assume H_P (section 3.3.1) = 2000 MeV/neutron

b - Assume H_P = 200 MeV/neutron

c - Assume $\sim 10^{14}$ cm^{-2} sec^{-1} fast neutron flux, 70 cm^2 D_2O scatterer, 10^4 rpm, 8 channels per rev., 2 slits per channel whence J_P (effective) = 2 x 70 x 10^{14} sec^{-1}

d - Assume chopper as in c and 9 x 10^{18} sec^{-1} continuous source strength whence J_P (effective) = 2 x 9 x 10^{18} sec^{-1}

e - Assume 1% of proton beam from storage ring is stopped in thin target, J_A=0.01x9x10^{18} sec^{-1}

f - Assume 1:100 microstructure pulses are deflected to a thin target stopping 1% of the beam, J_A = 0.01 x 0.01 x 9 x 10^{18} sec^{-1}.

in use today. However, as mentioned above, it is not yet clear that it will be practicable to devise a storage system that will accept the whole output of the S.O.C. and it may be necessary to settle for conversion of only a fraction of the c.w. output to pulses. It also may not be practicable to realize the full gain for the microstructure pulses because of neutron straggling and time-of-flight path-length uncertainties which limit the time resolution.

3.6.2.2 Thermal and Epithermal Neutron Intensities

In this section we shall compare the thermal and epithermal pulsed neutron flux intensities obtained with storage ring pulsing to that obtained under optimum conditions with continuous wave operation. Optimum conditions for cw operation are obtained with a large ($\geq$ 120 cm thick) D_2O moderator. The effective peak flux of neutrons in any pulse interval, defined by a mechanical chopper, in this mode of operation is equal to the time average value. On the other hand, with a pulsed neutron source, the neutrons emerging from the moderator are bunched together in time; the moderation process introduces some degree of blurring of the primary pulses, but there is in general an increase in peak neutron flux over the time average value. In making the comparison the following assumptions are made:

1. That the same time average neutron source strength is achieved in cw and storage ring pulsed operation.

2. That the requirement is for 5 μsec wide pulses 200 p.p.s., of either thermal (< 0.127 eV) or epithermal (0.127 < E < 1.46 eV) neutrons.

3. That in both modes of operation the neutron pulses are defined by a mechanical chopper. With the storage ring mode the chopper is phased with respect to the ring so that the 5 μsec long pulse is extracted from the peak of the neutron burst produced in the moderator.

A quantitative comparison of the peak fluxes for a variety of accelerator pulse widths, P, and for various moderator configurations is given in Fig. 6.1 in terms of an enhancement factor (E.F.) calculated from information in appendix 9. Here E.F. is the ratio of the effective neutron flux during the 5 μsec chopper pulse from the given moderator configuration to the neutron flux for optimum cw operation.

In calculating the values of E.F. for epithermal (thermal) neutrons it is necessary to find the quantities τ_E and $\phi_2(z,r)$ ($\tau_{0.127}$, τ_{th} and $\phi_{th}(z,r)$) defined in appendix 9 , for the moderator configurations considered. In a typical calculation we assume a moderator thickness R cm, with a small hole of depth (R-r) cm (Fig. 6.1) directed toward the center of the target. The calculation is necessarily inexact for several reasons. For example, the flux values ϕ can be found from appendix 9, on the assumption that presence of the beam hole produces no flux de-

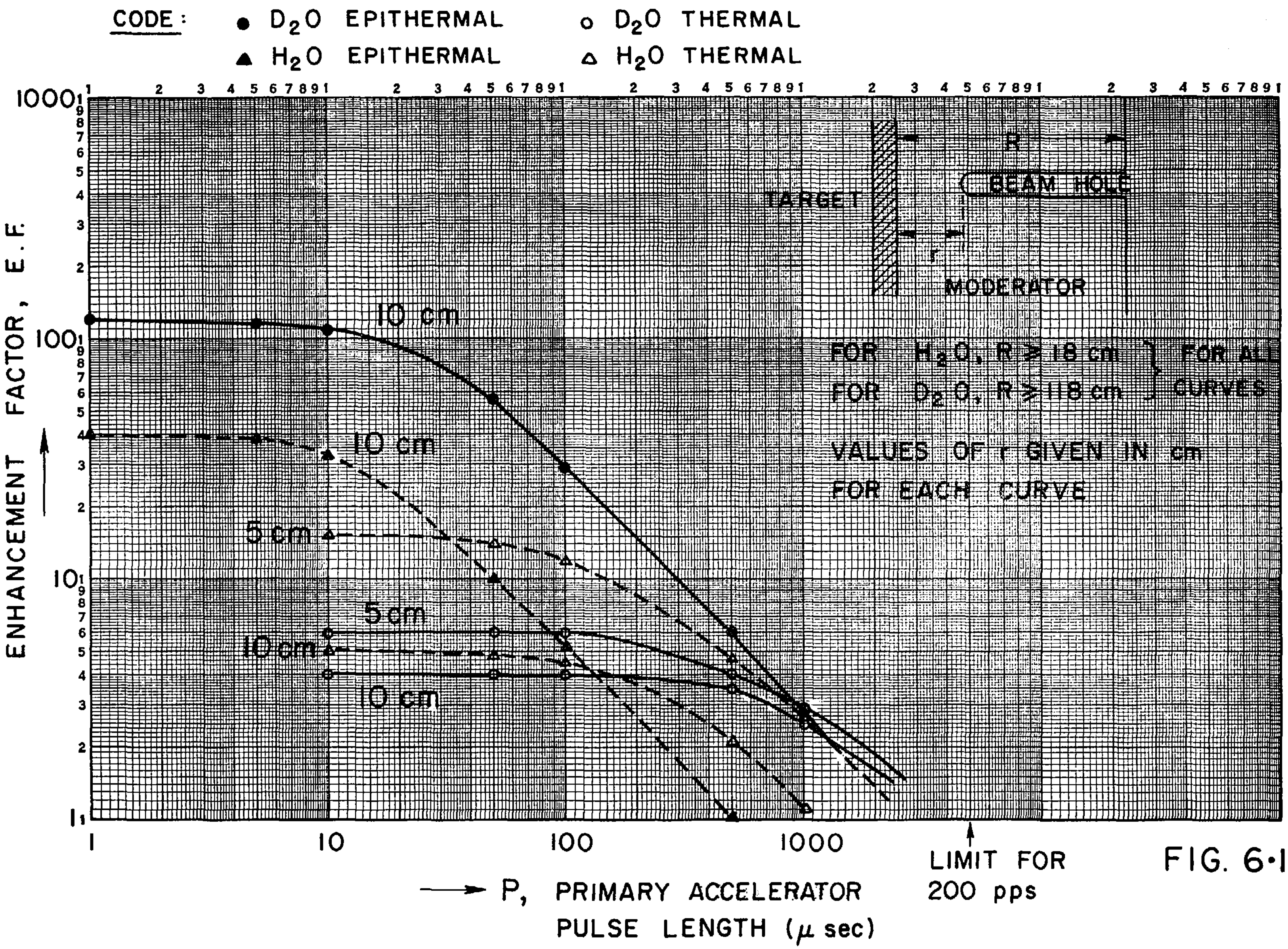
CODE:
● D_2O EPITHERMAL
○ D_2O THERMAL
▲ H_2O EPITHERMAL
△ H_2O THERMAL
ENHANCEMENT FACTOR, E. F.
P, PRIMARY ACCELERATOR PULSE LENGTH (μ sec)
1000
100
10
1
1
10
100
1000
10 cm
10 cm
5 cm
5 cm
10 cm
10 cm
TARGET
R
BEAM HOLE
r
MODERATOR
FOR H_2O, R ≥ 18 cm
FOR D_2O, R ≥ 118 cm
FOR ALL CURVES
VALUES OF r GIVEN IN cm FOR EACH CURVE
LIMIT FOR 200 pps

FIG. 6·1

pression. Furthermore, the precise dependence of the mean lives τ_E, $\tau_{0.127}$ and τ_{th} upon r and R has not been determined but only their dependence on R in the absence of beam holes. The E.F. values in Fig. 6.1 are based on plausible estimates of τ. For a wide range of conditions (e.g. for $P > 100$ μsec, or $r(D_2O) > 50$ cm, or $r(H_2O) > 12$ cm) these limitations are not serious because E.F. is not very sensitive to τ. However, for other conditions, e.g. $P < 50$ μsec, D_2O moderator and r small, the E.F. values are more uncertain. As an extreme example, for P = 10 μsec, r = 5 cm, D_2O, thermal neutrons, we obtain E.F. = 6^{+30}_{-3}.

Three conclusions may be drawn from Fig. 6.1 concerning accelerator and moderator design:

(i) There is little benefit to be gained by the provision of accelerator pulses shorter than about 10 μsec for neutrons with $E < 1.46$ eV.

(ii) Time-of-flight experiments employing thermal neutrons require an H_2O moderator for optimum operation, while many other experiments favour a large D_2O moderator. A composite moderator with separate H_2O and D_2O sections of various thicknesses, and provided with beam holes of various depths, would simultaneously fulfill the requirements of most proposed experiments.

(iii) Individual time-of-flight experiments employing epithermal (thermal) neutrons may benefit in intensity by about a factor 100 (10) if the neutron source is suitably pulsed. However, this gain is contingent on the practicability of converting the full cw beam to pulses with a storage ring.

3.7 Appendix 7

Target Room and Shielding

3.7.1 Possible Target Room Layout

A possible layout for a high neutron flux facility is shown in Fig. 3. The main proton beam from the S.O.C. accelerator would first pass through a meson target room and then to one of two neutron experimental areas or to a proton irradiation facility. Since most of the beam emerging from the thin meson producing target could be recovered (slightly degraded in energy, of course) meson and neutron or meson and proton experiments could be carried out simultaneously. Very short pulses of protons of 100 MeV energy could be removed from the accelerator to the short pulse experimental area for fast neutron time-of-flight experiments.

The main proton beam would be turned vertically downward by beam bending magnets before entering the neutron producing target assemblies as shown in Fig. 7.1. This geometry allows neutron beams to be taken out of the target assemblies in any horizontal direction while removing as many of the forward directed, high energy cascade neutrons from the experimental area as possible. Seven to ten feet of heavy concrete shielding would be required around the target assemblies to avoid undue activation of experimental equipment and high background levels in detectors. The two neutron experimental areas would be separated and shielded from each other so that maintenance and setting-up operations could be done in one while the other is in operation.

The activation problem from high energy neutrons could be alleviated by off-setting the neutron beam holes from direct view of the proton target. Beam holes at different horizontal levels could look at different moderator configurations and so give the neutron spectrum best suited to a particular experiment.

3.7.2 Shielding and Induced Radioactivity

The calculations of shielding requirements for the target assembly are necessarily approximate, because there is at present little experimental information on the absorption of high energy neutrons and the radio-activity induced by these neutrons. In our estimates we have used results reported at the 1st. International Conference on Shielding around High Energy Accelerators, held in France in 1962.

The present biological tolerance for high energy neutrons (> 200 MeV) is 2/sq. cm./sec.[48]. The half-thickness of ordinary concrete, heavy concrete and iron are approximately 18.0 in., 8.5 in. and 5 in. respectively[49]. In the proposed geometry the beam is incident downward on the target, which is surrounded by 10 ft. of heavy concrete. The shield around the target will be designed to reduce the number of fast evaporation neutrons and slow neutrons to a negligible level. According to Yale Report Y-6[(15)], the half intensity thickness of ordinary concrete increases from 10 in. to 18 between neutron energies of 100 to 200 MeV, while above 200 MeV the half intensity thickness remain nearly constant. Therefore in the present estimates we consider only cascade neutrons with energies >200 MeV.

For a total neutron production of 10^{19} neutrons/sec., the number of fast neutrons will be 2×10^{17} neutrons/sec. Because of the forward angular distribution of these neutrons[28] only 5%

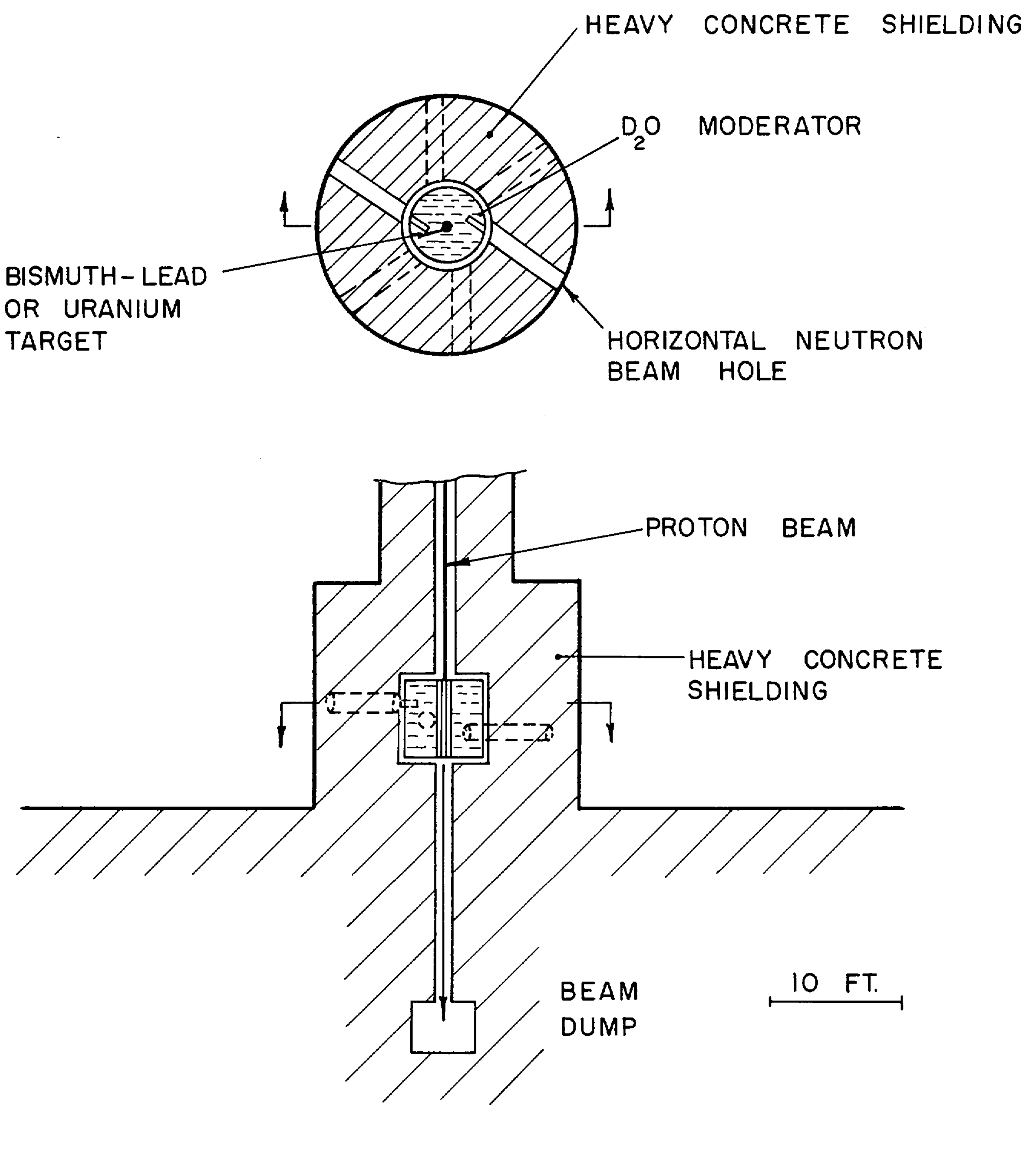

NEUTRON TARGET ASSEMBLY

FIG. 7·1

will enter the target area, i.e. $\sim 1 \times 10^{16}$; 10 ft. of heavy concrete will attenuate these by a factor of $\sim 10^5$ and so, at the outside face of shield around the target assembly, the flux will be $\sim 1 \times 10^5$/sq. cm./sec. This makes the experimental area inaccessible while the beam is on. In order to reduce the level outside the experimental area to less than the biological tolerance, a further shield of $\sim$ 25 ft. of ordinary concrete, or earth equivalent, will be required.

The fast neutron flux in the experimental area will induce radio-activity in the experimental equipment and the concrete walls of the building. Some measurements have been made on the induced activity in the vicinity of the CERN synchrocyclotron[50]. This machine operates $\sim$ 130-140 hours per week with a 0.8 μA beam of 600 MeV protons. The current in the present machine is $\sim 10^5$ times as great. However, the 10 ft. heavy concrete shield reduces the fast neutron flux by $\sim 10^5$ and so the problems associated with induced activity might be expected to be similar. Typical fields observed at CERN, 4-5 hours after shut-down, are $\sim$ 10-100 mR/hour at different locations in the target room. After 50 hours these would be reduced by a factor of $\sim$ 3, but at longer times the decay rate was much slower ($t_{1/2}$ $\sim$25 days).

In the present machine, we would expect similar radiation fields to exist a few hours after shut-down. By suitable choice of construction materials for experimental apparatus, one could probably reduce the level of activity. If a water barrier was used as the first part of the biological shield outside the experimental area, the level due to activation in the materials is the concrete could be substantially reduced. Before detailed predictions can be made, more experimental information is required. This could be obtained from experiments at machines already operating at much lower currents.

3.8 Appendix 8

High Energy Experiments

3.8.1 Introduction

Over the past few years there has been a large effort devoted to the design and development of so-called "meson factories". All accelerators listed in Table II, Appendix 4 are intended for this purpose. The proton beam from the accelerator as discussed in the present report would be a much more powerful tool for meson research than any of the hitherto proposed machines. With a 60 ma beam of 750 MeV protons, it would produce, from a thin target, 10 to 10^2 times as many mesons as the proposed meson factories (Appendix 4), and 10^2 to 10^3 times as many mesons as any high energy accelerator operating at present.

In the following discussions it is assumed that the accelerator will deliver 60 ma of protons at 750 MeV, an energy for which meson yields are directly available[15,16]. At 970 MeV the yields would be substantially greater; the question of optimum beam energy is discussed in section 3.8.4.

The list of high energy experiments below contains a number of experiments, properly classified as belonging to the field of nuclear structure, in which beams of muons and pions are used as probes for studying the nucleus. These particles have very different mass, interaction properties, spin and isotopic spin from the particles currently used to investigate nuclei and many new effects are to be expected. Many interesting experiments, presently unforseen will undoubtedly be made possible by the accelerator.

3.8.2 Beams Available from the Accelerator

Table VII lists the kinds and intensities of secondary beams which may be obtained. The estimates are derived mainly from Yale reports[15,16].

3.8.3 Possible Experiments

A summary of some of the experiments that would be possible with these beams follows. Since many of these experiments are considered feasible for only a small fraction of a 1 ma beam[15], it should be possible to run them as parasitic experiments on the S.O.C., taking only 0.1 to 1% of the beam pulses. However, of equal importance will be high precision experiments using different techniques from those now in use and the search for rare processes. The latter may require up to say 20% of the full beam current.

3.8.3.1 Experiments Considered Feasible by Outside Laboratories

The following list of experiments was compiled by the Yale study group[15]:-

I. Intrinsic Properties of Particles; Electromagnetic Interactions

(1) Muon mass, using mesic x-rays and crystal spectrometer.

(2) Muon magnetic moment relative to proton magnetic moment, using gas target to avoid diamagnetic uncertainties.

Table VII

Beam	Energy (MeV)	Source	Collector Solid Angle (Ster.)	Distance from Target	Intensity (No. /Sec.)
Pi Mesons					
$\pi+$	200±1%	C target, $6g/cm^2$	10^{-4}	30 ft	7.2×10^9
$\pi+$	400±1%	C target, $6g/cm^2$	10^{-4}	30 ft	3.6×10^9
$\pi-$	200±1%	C target, $6g/cm^2$	10^{-4}	30 ft	1.0×10^8
$\pi-$	400±1%	C target, $6g/cm^2$	10^{-4}	30 ft	5×10^8
$\pi+$	200±10%	Al target, $20g/cm^2$	10^{-2}	80 ft	2.4×10^{12}
$\pi+$	400±10%	Al target, $20g/cm^2$	10^{-2}	80 ft	1.2×10^{12}
$\pi-$	200±10%	Al target, $20g/cm^2$	10^{-2}	80 ft	3.6×10^{11}
$\pi-$	400±10%	Al target, $20g/cm^2$	10^{-2}	80 ft	1.8×10^{11}
Mu Mesons					
$\mu+$	125±1%	250 MeV $\pi+$ decay		130 ft	3×10^{10}
$\mu+$	400±1%	400 MeV $\pi+$ decay		130 ft	2.4×10^9
$\mu-$	125±1%	250 MeV $\pi-$ decay		130 ft	4×10^9
$\mu-$	400±1%	400 MeV $\pi-$ decay		130 ft	3×10^8
Stopped $\mu+$	0	Stopping target 4 in^2, $6g/cm^2$			3×10^9
Stopped $\mu-$	0	Stopping target 4 in^2, $6g/cm^2$			3.6×10^8
Neutrinos					
ν_μ	30	Stopped $\pi+$		50 ft	6×10^8
$\nu_\mu + \nu_e$	~90(total)	Stopped $\mu+$		50 ft	6×10^8
ν_μ	90	Captured $\mu-$		~150 ft	$> 5 \times 10^7/cm^2$
ν_μ	125-240	$\pi+$ decay in flight		~150 ft	$> 5 \times 10^7/cm^2$
$\bar{\nu}_\mu$	125-240	$\pi-$ decay in flight		~150 ft	$> 5 \times 10^6/cm^2$
ν_e	~ 1	Bi target (p, xn) reactions, followed by K capture		~150 ft from neutron target	$\gtrsim 10^9/cm^2$
$\bar{\nu}_e$	~ 1	Bi target, reactions followed by β decay		~150 ft from neutron target	$\sim 10^9/cm^2$
Neutrons	200-750	Bi target, 400 gm/cm^2	~0° to proton beam	50 ft	$\sim 3 \times 10^9/cm^2$

(3) Muon g-value, g-2 experiment.

(4) Muonium energy levels, in particular the hyperfine structure of the ground state for the precise determination of α; Lamb shift in $n = 2$ states; use of low pressure gas targets.

(5) Pion mass, using mesic x-rays and crystal spectrometer.

(6) Mass of ν_μ from m_π, m_μ and accurate decay spectrum.

(7) Vacuum polarization, using mu mesic x-rays and crystal spectrometer.

II. Weak Interactions

(1) Muon capture in H and D, including measurement of neutron polarization; use of gas target to avoid atomic and molecular complications.

(2) Muon decay spectrum, precision measurement to look for effect of intermediate boson.

(3) Radiative muon capture: $\mu^- + p \rightarrow n + \nu_\mu + \gamma$ (relativistic, pseudoscalar, and weak magnetism effects).

(4) Rare decay modes of muon.

(5) Search for new weak interaction coupling muonium and antimuonium.

(6) Beta decay of pion: $\pi^+ \rightarrow \pi^0 + e^+ + \nu_e$.

(7) Radiative pion decay: $\pi^+ \rightarrow \mu^+ + \nu_\mu + \gamma$ to measure mass of ν_μ.

(8) Branching ratio $(\pi^+ \rightarrow \mu^+ + \nu_\mu)/(\pi^+ \rightarrow e^+ + \nu_e)$ to study universality of Fermi interaction.

(9) Neutrino induced reactions. Some energetically possible reactions are:

(i) $\bar{\nu}_e + p \rightarrow e^+ + n$ (Cowan - Reines experiment)

(ii) $\nu_e + n \rightarrow e^- + p$ (Cl^{37} experiment)

(iii) $\nu_\mu + n \rightarrow \bar{\mu} + p$

(iv) $\bar{\nu}_\mu + p \rightarrow \mu^+ + n$

(v) $\bar{\nu}_\mu + p \rightarrow n + e^+ + \pi^o$

(vi) $\bar{\nu}_\mu + p \rightarrow \Lambda^o + e^+$

III. Strong Interactions

(1) Nucleon-nucleon scattering. Systematic investigation of differential cross section over wide energy range for both elastic and inelastic processes.

(i) Double and triple scattering

(ii) p - p scattering

(iii) n - p scattering

(iv) Double pion production $p + p \rightarrow 2n + 2\pi^+$ (near threshold)

(2) Pion-nucleon scattering

(i) Systematic, precise investigation of differential elastic scattering cross sections, including use of polarized targets and measurements of recoil polarization.

(ii) Pion-nucleon inelastic scattering $\pi^+ + p \rightarrow \pi^+ + \pi^+ + n$ to study pion-pion interaction.

(3) Neutron-neutron interaction $\mu^- + d \rightarrow n + n$ (muon capture by deuteron).

(4) Non-associated production $p + n \rightarrow \Lambda^0 + p$.

IV. Nuclear Structure

The following list of experiments contains suggestions from the Yale study[15] and from a study carried out at Los Alamos[17]:-

(1) Mu meson experiments

(i) Mu-mesic x-rays to determine nuclear electric quadrupole moments and polarizability using high resolution spectrometer.

(ii) Mu-capture to learn about the induced pseudo-scalar coupling constant and about the properties of nuclear wave functions (e.g. N^{16}) not easily reached by other means.

(iii) Mu-scattering (elastic and inelastic) - possible advantages over electron scattering experiments are

(a) less bremsstrahlung, (b) better energy resolution (resulting from heavier mass) unabling better determination of the charge distribution (c) both charges almost equally abundant (d) polarization of the mass.

(iv) (μ,n) reactions with $\sim$ zero neutrino energy yielding information about direct nuclear reactions.

(2) Pion experiments

Like nucleons the pions interact strongly with the nucleus but offer some distinct advantages over nucleons:

(a) no exclusion principle complicating the reaction

(b) less orbital angular momentum at the same energy

(c) large mean free path at low energies allowing better identification of single-collision processes. Some experiments are:-

(i) Spin-flip reactions

(ii) Excitation of isobaric analogue states that cannot be reached by other means.

(iii) Pion absorption yielding information on clustering of nucleons

(iv) Pion-nucleus scattering to study nucleon distributions in the nucleus

(3) Proton-Nucleus Scattering

(i) Quasi-elastic scattering such as (p,2p), (p,d) and (p,2n) to determine nucleon momenta in the nucleus and nuclear orbital structure.

(ii) Scattering of polarized protons by nuclei to study spin-orbit interaction.

3.8.3.2 Initial C.R.N.L. Experiments

The following have been suggested as feasible initial experiments.

I. New nuclides produced by spallation reactions in the target would be of interest for decay scheme studies. These nuclei are very neutron deficient, and lie in a region of the periodic table at present inaccessible. Cross sections are reported in the range ~ 1 to 50 mb[51,52]. The combination of the high current accelerator, the isotope separator, and the high resolution β-spectrometer should make possible the study of many neutron-deficient isotopes, some a long way from the stability line. A limitation would be in the half lives of the nuclei so formed.

II. The experiments listed in Part I of Section 3.8.3.1, although requiring a high energy machine for meson production, are essentially low energy experiments employing in some cases technique already well developed at C.R.N.L., e.g. crystal diffraction spectrometry. The use of low-pressure gas targets to avoid atomic perturbing effects would be facilitated by the large beam intensities proposed.

III. The scattering experiments listed in Part III of Section 3.8.3.1, viz. p-p, n-p, pion-nucleon, and multiple scattering, would entail extensions of experimental techniques already available at C.R.N.L. For measurements of polarization parameters in p-p scattering, the accelerator would provide sources from 10 to 100 times stronger, at a given energy, than any existing machine (see for example ref. 53). If, in addition, a variety of proton beam energies were available, the usefulness of the facility would be enhanced accordingly.

IV. Because it will be possible to obtain intense pulses of fast neutrons having a wide energy spread, time-of-flight techniques can be used to study neutron scattering as a function of energy. It should be possible to study n-p angular distributions and polarizations near 200 MeV with a precision at present obtainable only for proton scattering.

3.8.4 Energy Considerations

The best energy for a meson factory, from the experimental point of view, has been discussed by Edge and co-workers[54]. The minimum energy giving useful densities of stopped π mesons and adequate beams of high energy mesons and neutrinos is in the region of 450 to 500 MeV. There would appear to be no strong criterion for selecting any particular maximum value of proton energy; the best energy would be the highest possible. However, it may be of value to note that for energies below 1000 MeV, relatively pure pion beams are available, the only contaminants being μ-mesons and electrons.

For most of the experiments listed in 3.8.3.1 Parts I and II, excepting the neutrino experiments, there does not seem to be much advantage in having high proton (hence pion) energies. On the other hand, for the strong interaction and nuclear structure experiments, 3.8.3.1 Parts III and IV, there is much to be gained by being able to vary the proton energy over a wide range.

3.8.5 Possible Future Extension of Facility

The large production of pions, both positive and negative, raises the possibility[55] of further accelerating these particles in an auxiliary accelerator. In order to be useful such an accelerator should raise the pions to $\gtrsim$ 1000 MeV. This would require $\gtrsim$ 800 MeV of post-formation acceleration. This facility would make almost all the pion-nucleon and mesic resonant states classified as δ, α, ψ, ζ, η, and ϕ[56], and the charged Σ particles (hypersons) accessible to experiment under relatively ideal conditions.

3.9 Appendix 9

Neutron Moderation Calculations

3.9.1 Method of Calculation

Neutron fluxes and lifetimes for various neutron energies and target-moderator assemblies have been carried out by S. Kushneriuk[57]. In this appendix we define the quantities which have been calculated and give those results of most direct interest to the target-moderator assembly considered in appendices 5 and 6.

The neutron flux and lifetime in the assembly depends on: (a) the neutron yield by the proton bombarded target, (b) the primary energy spectrum of these neutrons, (c) the range of energies of the group of neutrons being considered, (d) the target material, (e) target length, (f) target size, (g) nature of the moderator, (h) the moderator size and (i) position in the moderator.

In the calculations carried out, the target-moderator assembly and the primary neutron source disposition were taken to be the following: the target is a cylinder of radius b, length h and the moderator surrounding the target is a cylindrical sheath of thickness (R-b) and length H. Neutron sources of strength Q per cm length of target per sec were uniformly distributed through the target.

The coordinates Z and r are used to denote axial and radial distances in this cylindrically symmetrical system. Z = 0 defines the mid plane intersecting the system and the system is taken to be symmetrical about this plane.

The quantities specifically calculated were:-

$\phi_F(Z,r)$; the first flight collision distribution of the source neutrons in the moderator.

$\phi_1(Z,r)$ and $\phi_2(Z,r)$; two-group "diffusion"-type fast and epithermal neutron flux distributions in the moderator. The group $\phi_2(Z,r)$ consists of neutrons with energies in the range $0.127 \text{ eV} < E < 1.46 \text{ eV}$ and the energy spectrum of this flux is roughly a 1/E-type spectrum.

$\phi_{th}(Z,r)$; a one-group diffusion-type thermal neutron flux distribution, the energy spectrum of the neutrons within this group being roughly Maxwellian.

$J_1(Z,R)$, $J_2(Z,R)$ and $J_{th}(Z,R)$; the current of neutrons for the respective groups at the outer face of the moderator, i.e. at $r = R$.

For further details of the energy spectrum of the neutrons encompassed by each group defined above see ref. 57. A few auxiliary quantities such as the mean neutron life in the system, τ, the mean life of thermal neutron in the system, τ_{th}, and the mean time for the neutron to reach energy E, $\tau(E)$, were also calculated.

3.9.2 Results of Calculation

Typical results of the calculations are shown in Figs. 9.1 to 9.8. A more complete set of results is given in Ref. 57. The results shown here are the ones used in appendices 5 and 6 and they also serve to illustrate how the factors (a) to (i) affect the neutron flux.

Note first that, since the primary neutron source strength, Q, is taken to be uniformly distributed throughout the target, all neutron flux and current values are directly proportional to Q.

The calculations were performed for primary neutron energy spectra resulting from bombardment of the target by protons of about 800 MeV energy*. The primary spectrum, for a given target, is represented in general terms as the sum of three components.

$$N(E) = N_T \left[f_F\, n_F(E) + f_e n_e(E) + f_c n_c(E)\right] \qquad (9.1)$$

in which N_T is the total neutron yield per proton entering the target, $n_F(E)$ is the spectrum of neutrons released in the target fission processes, $n_e(E)$ is a neutron evaporation spectrum and $n_c(E)$ is the neutron emission spectrum in particle cascade interactions. The f's are the relative weights assigned to each of

* Negligible error is introduced by applying the same neutron spectrum to a bombarding energy of 970 MeV.

the spectra. Specifically $n_e(E)$ is an evaporation spectrum,

$$n_e(E) = (E/\tau^2) \exp(-E/\tau)$$

in which τ is an effective nuclear temperature for the evaporation process. For target materials in which fission is significant the Maxwellian representation

$$n_F(E) = (4E/\pi\tau_F{}^3)^{1/2} \exp(-E/\tau_F),$$

was used. $n_c(E)$ was presented graphically. For bismuth and lead targets and 800 MeV incident protons, f_F, f_e, f_c, τ and τ_f had the values 0, 0.82, 0.18, 3.2 and 1.29 MeV respectively.

The spectrum of equation 9.1 does not take account of modifications in the neutron energy due to inelastic collisions of neutrons with the target nuclei. Inelastic collision effects were therefore incorporated into the calculations so that the spectrum of neutrons actually leaving the target is different from eqn. 9.1.

It should be pointed out that in large D_2O (and H_2O) moderated assemblies, the magnitude of the thermal neutron flux near the target is quite insensitive to the exact details of the spectrum N(E) but depends rather on N_T. On the other hand, if moderator layers are thin, the details of the energy of the emitted neutrons become more important. For thinly moderated assemblies with the same N_T, a revised spectrum* which is generally less

* A more precise representation of the spectrum is currently being calculated[22].

energetic than that given by eqn. (9.1) should result in neutron fluxes which are somewhat larger than the values quoted here.

3.9.3 Discussion of Results

It is evident from Figs. 9.1 to 9.3 , that the neutron fluxes and currents attained in each of the groups considered and the mean neutron lifetimes in the system, depend intimately on the moderator material and size. It is clear that if it is of interest for a particular application to use neutrons that come directly from the outer surface of the moderator, the moderator thickness must then be chosen to give maximum current for the type of neutron spectrum desired. If in addition it is desired that the mean neutron life in the system be small, then thin H_2O moderated systems would appear to be the best choice. If high fluxes over fairly large volumes are desired, then large D_2O moderators are needed. It may be noted from figure 9.1 that a H_2O moderator thickness of about 18 cms is effectively infinite in so far as neutron flux values, ϕ_1 and ϕ_{th}, at the target surface, are concerned. From figure 9.2 we see that $\phi_{th}(0,b)$ is still increasing for D_2O moderator thickness near to 90 cms; in fact for this particular target (i.e. h = 33 cms, Q = 10 n's/cm sec) the maximum flux attained at r = b, Z = 0 is about 1.5 n's/cm^2 sec. The mean neutron lifetimes in these large systems may be of interest (Fig.9.4). In a large H_2O moderated assembly the mean life is about 230 μsec of which 15 μsec is the average slowing down time, 215 μsec is the mean thermal life. The values for "infinite" D_2O moderated assemblies are 6.1×10^4 μ sec for the mean life, 50 μsec for the slowing down time. The short mean thermal life in large H_2O moderated systems is, of course, due to the relatively large thermal neutron capture cross section in H_2O.

The flux profile in D_2O moderated systems as well as the effect of varying the thickness of the moderator upon the flux are further illustrated on Figs. 9.5 and 9.6 . To obtain fluxes close to the optimum flux discussed in section 3.5.2 the thickness of the D_2O must exceed 100 cm.

The effect of different target materials is illustrated in Fig. 9.7 which compares thermal fluxes for "uranium" and bismuth targets. The "uranium" is depleted uranium so that thermal neutron fission is negligible. The differences in the results between the Bi and uranium targets of the same radius and the same source strength (as in Fig. 9.7) are due primarily to the fact that uranium absorbs thermal neutrons while Bi is essentially transparent to thermal neutrons. The flux profile curves for uranium corresponding to the curves given in Fig. 9.5 for bismuth are not shown but in a general way (because of thermal neutron absorption by the uranium) they are similar in shape to the HFBR curve of Fig. 9.5 . As mentioned, the comparison in Fig. 9.7 is made for bismuth and "uranium" targets with equal source strength. For a given proton beam current the choice of target (see appendix 5) is affected by the actual neutron yield from the target and the heat production in the target.

The effect of target radius on the thermal neutron flux can be seen in Figs. 9.6 and 9.7 . The effect of target length on the thermal neutron flux is shown in Fig. 9.8 . The roughly linear increase of the neutron flux for target lengths of up to approximately 60 cms arises because of the rather large spread of the first flight collision distribution, $\phi_F(Z,r)$, in the Z direction (even for short targets) combined with the fact that the migration length for neutrons in a D_2O moderator is large ($\sim$ 100 cm). Note that the plot in Fig. 9.8 is for a bismuth target and a thick D_2O moderator. This plot would not apply to thin moderators (where neutron leakage out of the system is a dominating effect) nor to targets which strongly absorb thermal neutrons (i.e. where leakage into the target is important). The dependence of the neutron flux on the target radius and target length is influenced by the migration area of the neutrons in the moderator surrounding the target and therefore Figs. 9.6, 7 and 8 do not apply to H_2O moderator assemblies.

FIGURE 9·1

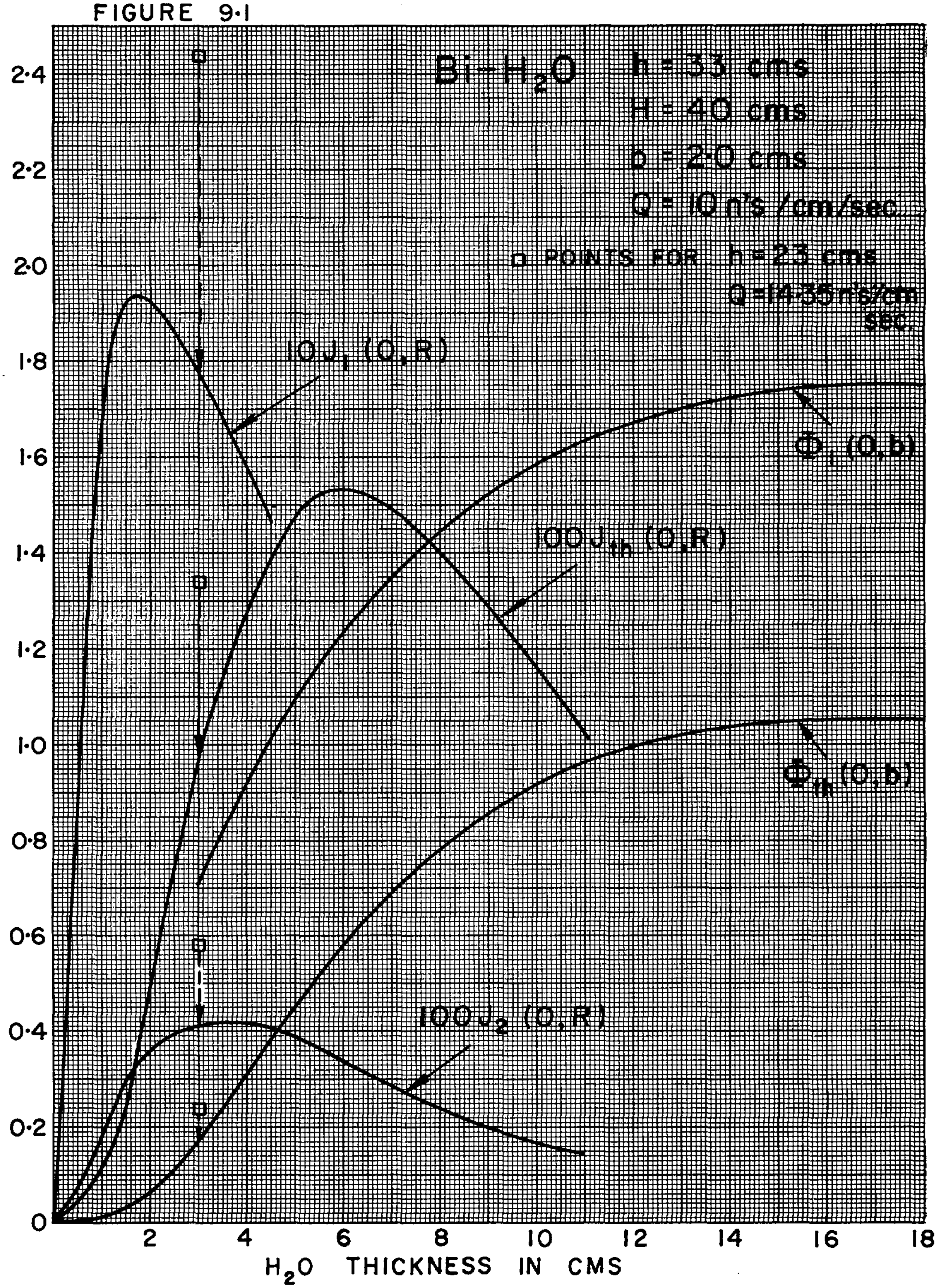
Bi-H2O
h = 33 cms
H = 40 cms
b = 2·0 cms
Q = 10 n's /cm/sec.
□ POINTS FOR h = 23 cms
Q = 14·35 n's/cm sec.
10 J1 (O, R)
Φ1 (O, b)
100 Jth (O, R)
Φth (O, b)
100 J2 (O, R)
0
0·2
0·4
0·6
0·8
1·0
1·2
1·4
1·6
1·8
2·0
2·2
2·4
2
4
6
8
10
12
14
16
18
H2O THICKNESS IN CMS

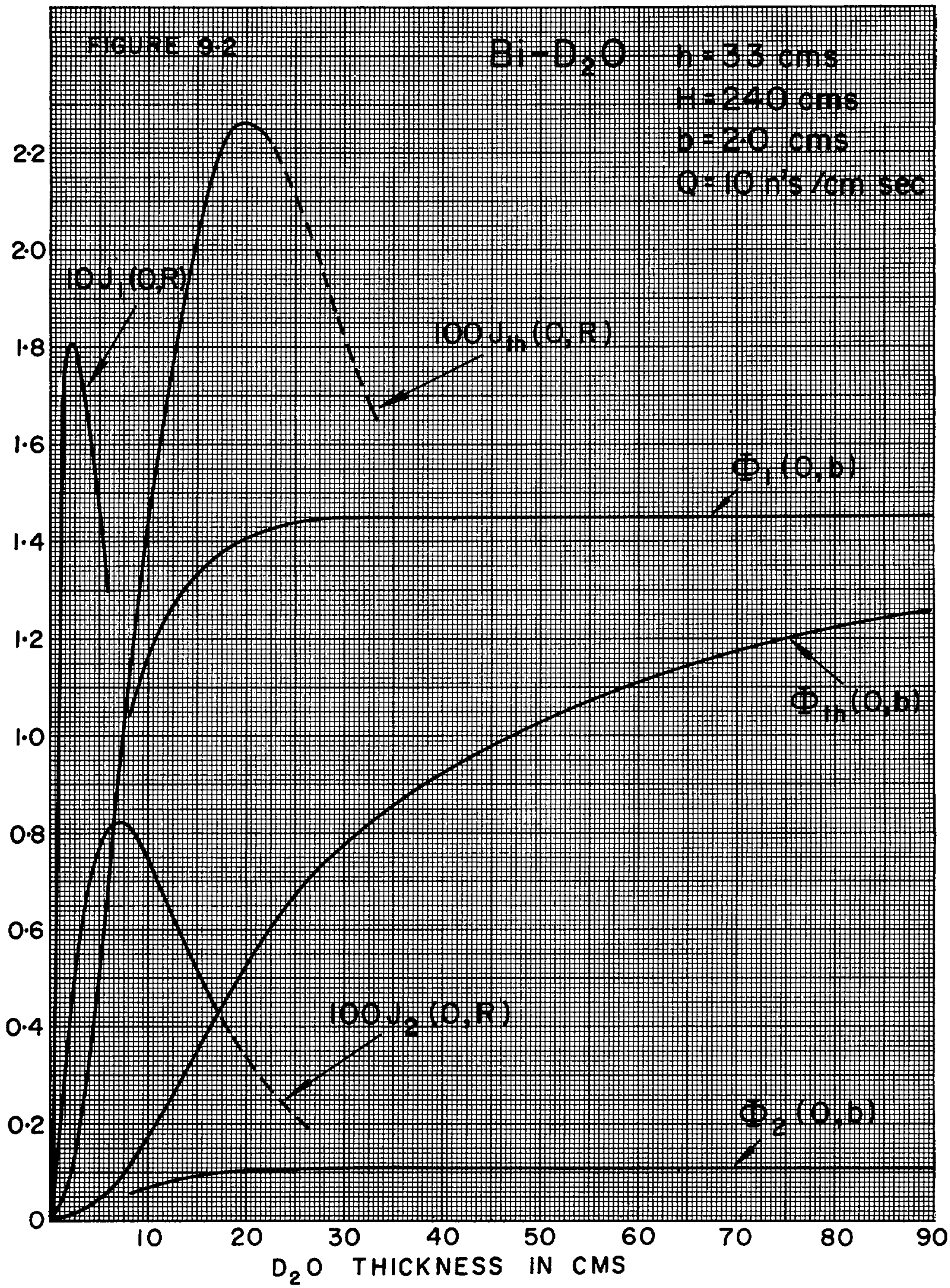

FIGURE 9·2
Bi-D₂O
h = 33 cms
H = 240 cms
b = 2·0 cms
Q = 10 n's/cm sec
10 J₁ (O,R)
100 Jₜₕ (O,R)
Φ₁ (O,b)
Φₜₕ (O,b)
100 J₂ (O,R)
Φ₂ (O,b)
0
0·2
0·4
0·6
0·8
1·0
1·2
1·4
1·6
1·8
2·0
2·2
10
20
30
40
50
60
70
80
90
D₂O THICKNESS IN CMS

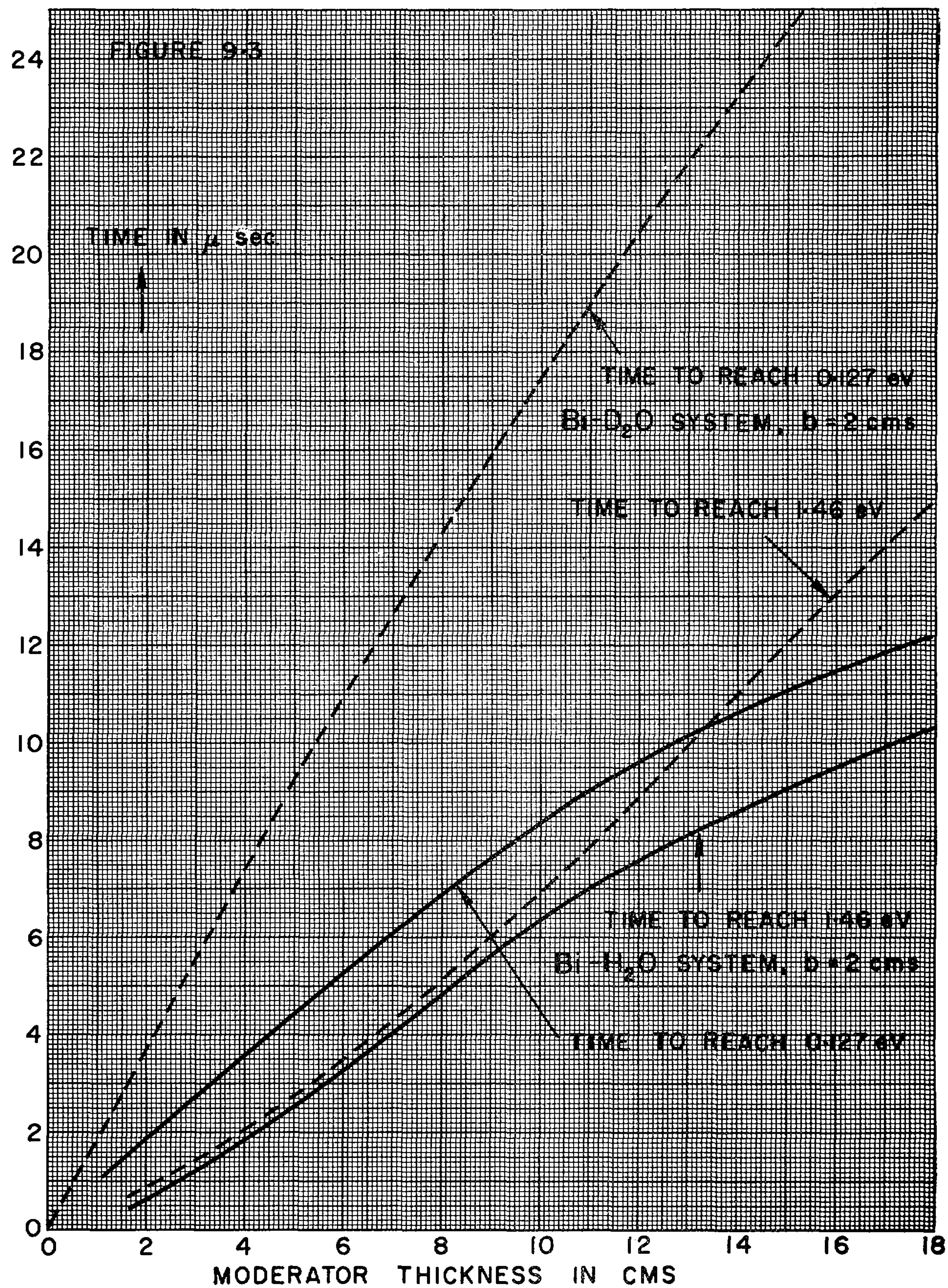

FIGURE 9·3
TIME IN μ sec
TIME TO REACH 0·127 eV
Bi-D2O SYSTEM, b = 2 cms
TIME TO REACH 1·46 eV
TIME TO REACH 1·46 eV
Bi-H2O SYSTEM, b = 2 cms
TIME TO REACH 0·127 eV
0
2
4
6
8
10
12
14
16
18
20
22
24
MODERATOR THICKNESS IN CMS

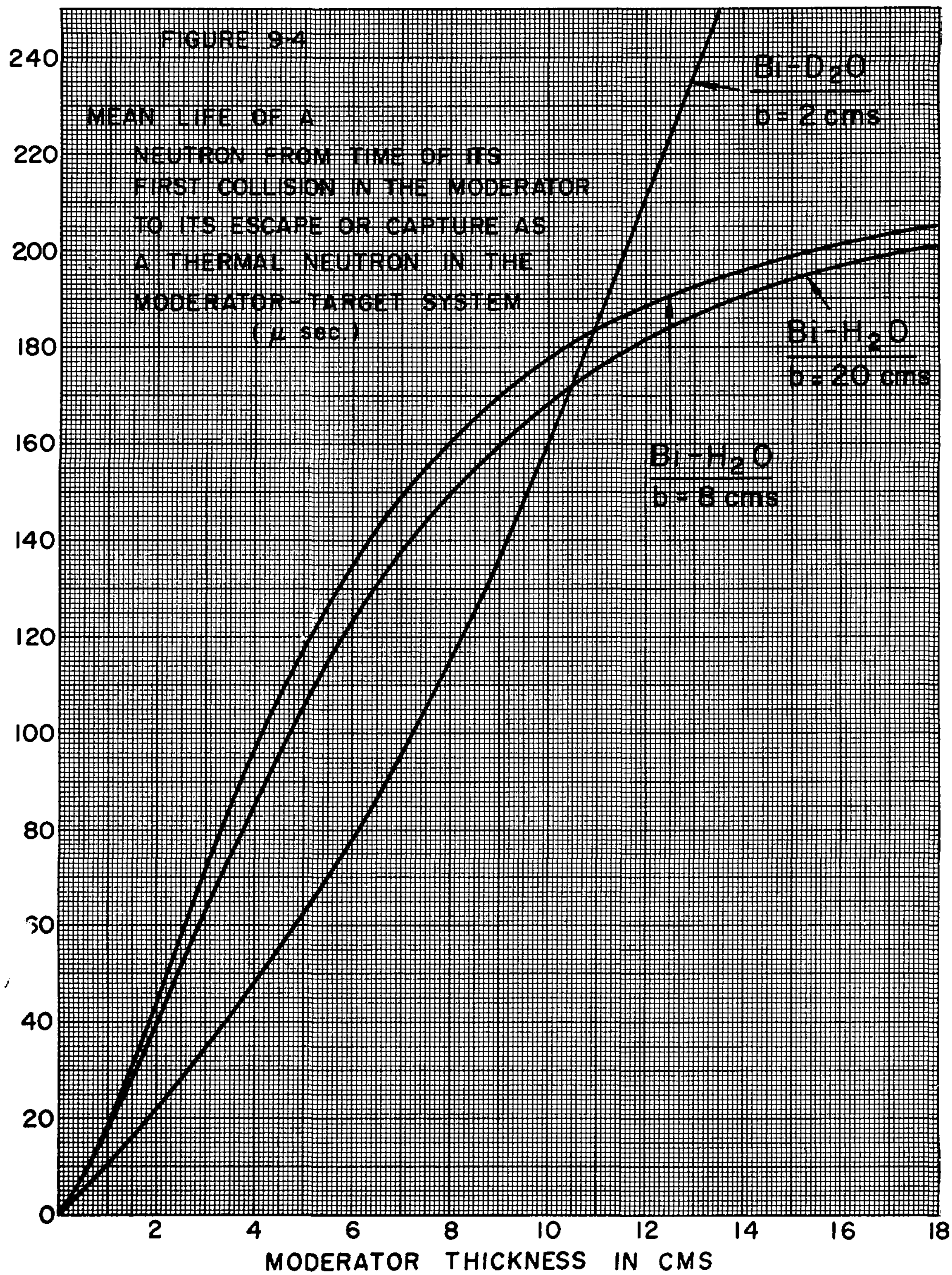

FIGURE 9-4
MEAN LIFE OF A NEUTRON FROM TIME OF ITS FIRST COLLISION IN THE MODERATOR TO ITS ESCAPE OR CAPTURE AS A THERMAL NEUTRON IN THE MODERATOR-TARGET SYSTEM (μ sec)
Bi-D_2O b = 2 cms
Bi-H_2O b = 20 cms
Bi-H_2O b = 8 cms
0
20
40
60
80
100
120
140
160
180
200
220
240
2
4
6
8
10
12
14
16
18
MODERATOR THICKNESS IN CMS

FIGURE 9·5

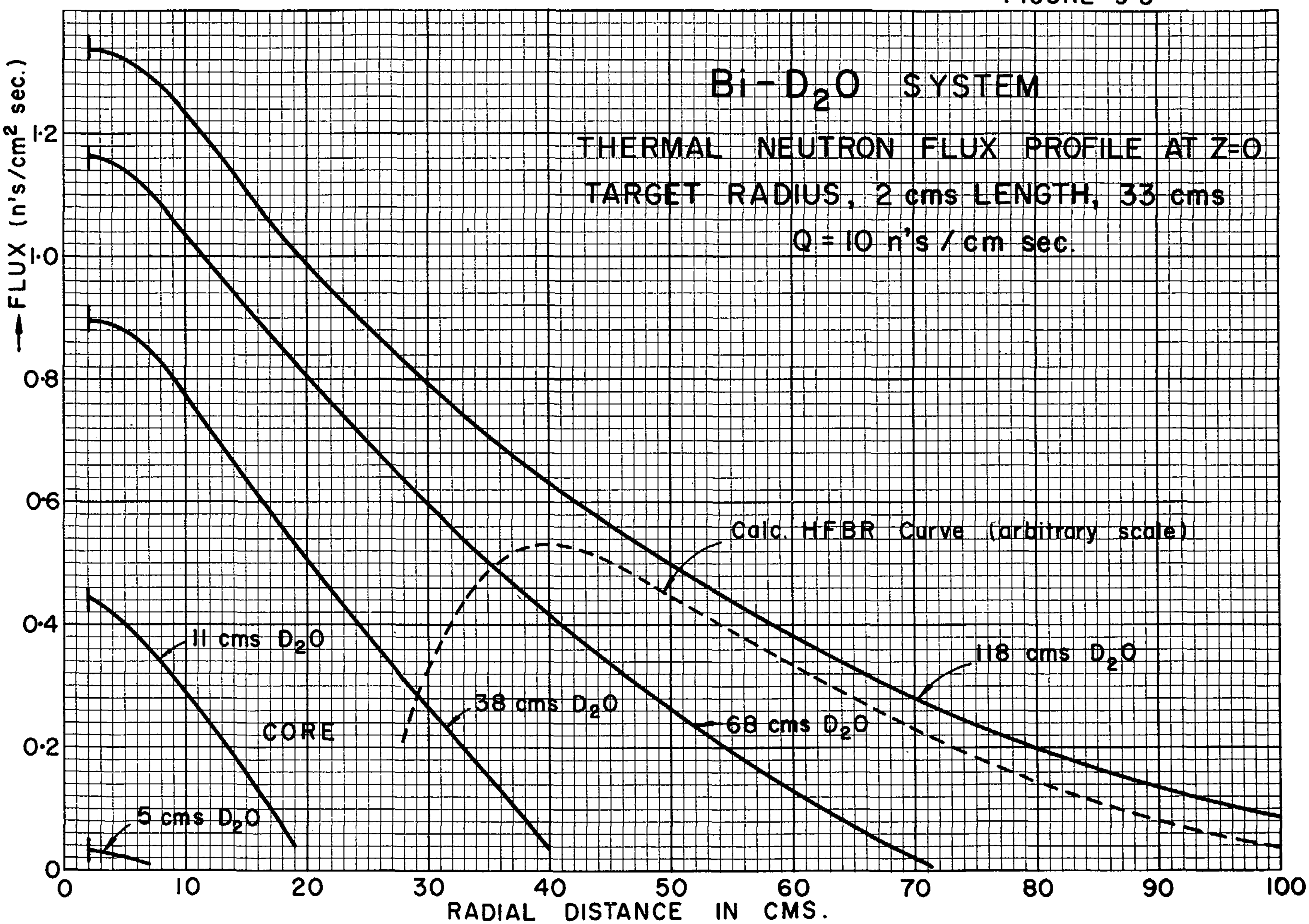
Bi-D_2O SYSTEM
THERMAL NEUTRON FLUX PROFILE AT Z=O
TARGET RADIUS, 2 cms LENGTH, 33 cms
Q = 10 n's / cm sec.
FLUX (n's/cm² sec.)
1·2
1·0
0·8
0·6
0·4
0·2
0
Calc. HFBR Curve (arbitrary scale)
11 cms D_2O
118 cms D_2O
38 cms D_2O
68 cms D_2O
CORE
5 cms D_2O
0
10
20
30
40
50
60
70
80
90
100
RADIAL DISTANCE IN CMS.

FIGURE 9·6

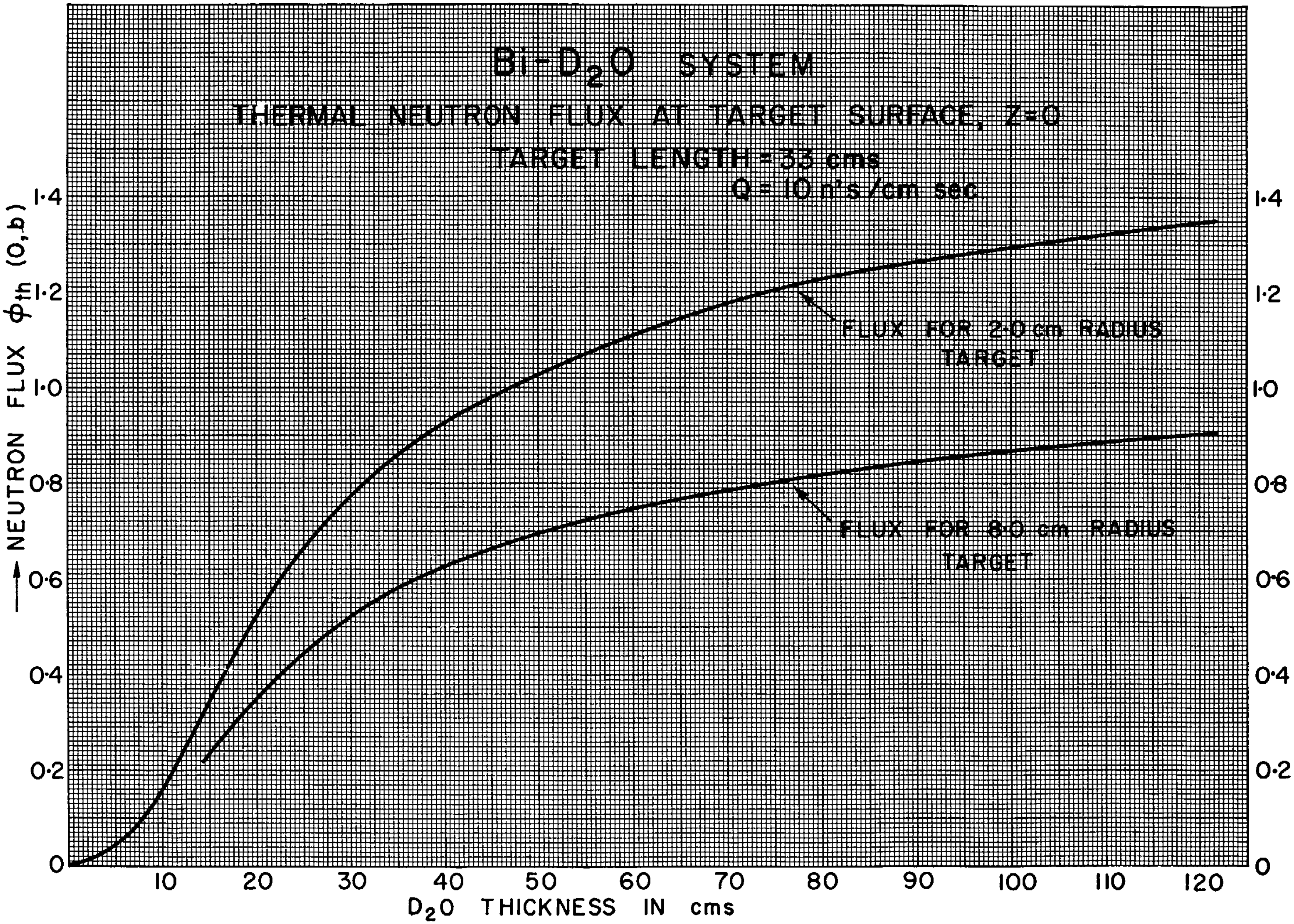
Bi-D_2O SYSTEM
THERMAL NEUTRON FLUX AT TARGET SURFACE, Z=O
TARGET LENGTH = 33 cms
Q = 10 n's /cm sec.
FLUX FOR 2.0 cm RADIUS TARGET
FLUX FOR 8.0 cm RADIUS TARGET
NEUTRON FLUX ϕ_{th} (0,b)
D_2O THICKNESS IN cms
0
0·2
0·4
0·6
0·8
1·0
1·2
1·4
10
20
30
40
50
60
70
80
90
100
110
120

FIGURE 9·7

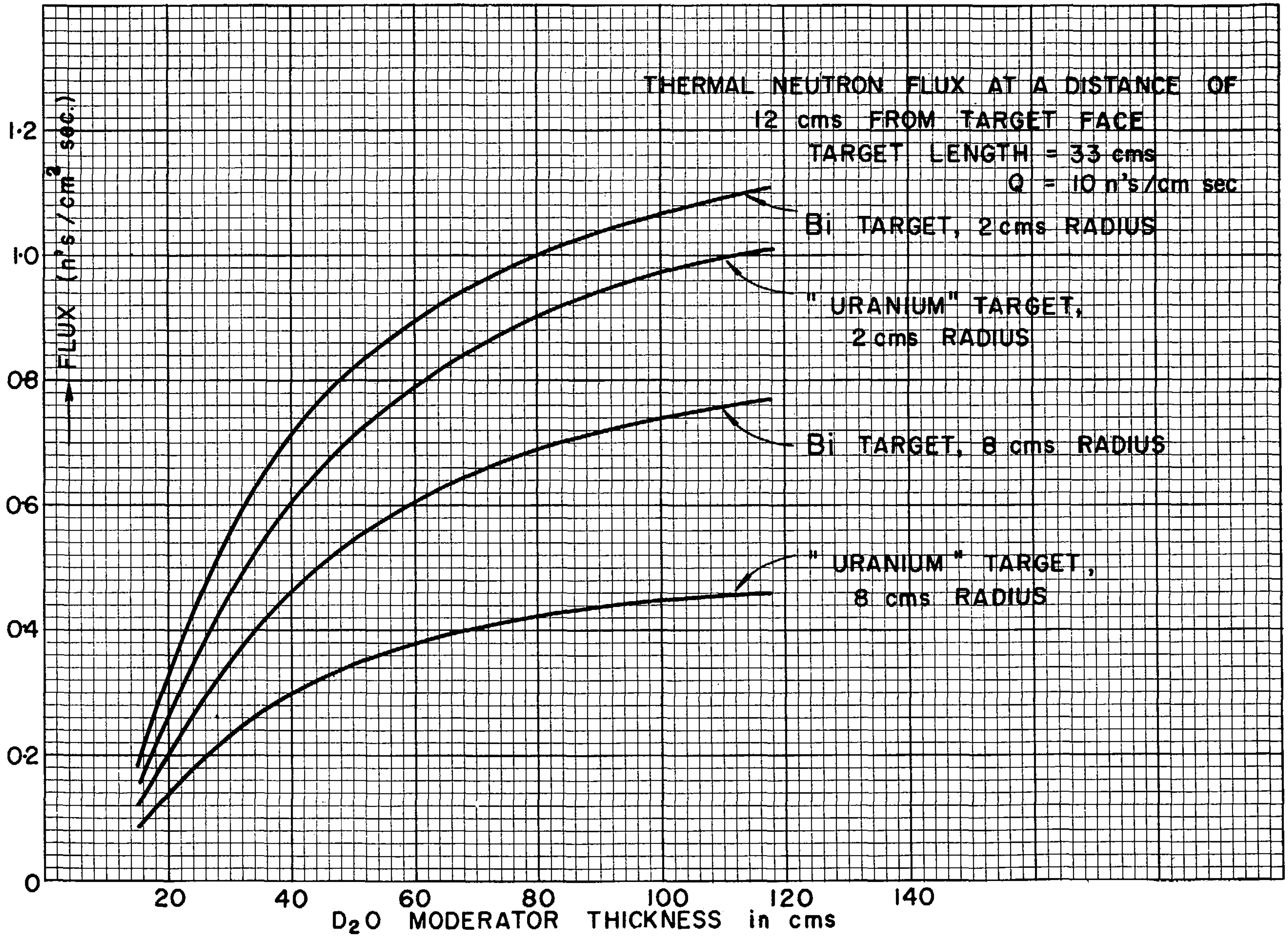

THERMAL NEUTRON FLUX AT A DISTANCE OF
12 cms FROM TARGET FACE
TARGET LENGTH = 33 cms
Q = 10 n's/cm sec
Bi TARGET, 2 cms RADIUS
" URANIUM" TARGET,
2 cms RADIUS
Bi TARGET, 8 cms RADIUS
" URANIUM " TARGET,
8 cms RADIUS
FLUX (n's/cm² sec.)
1·2
1·0
0·8
0·6
0·4
0·2
0
20
40
60
80
100
120
140
D₂O MODERATOR THICKNESS in cms

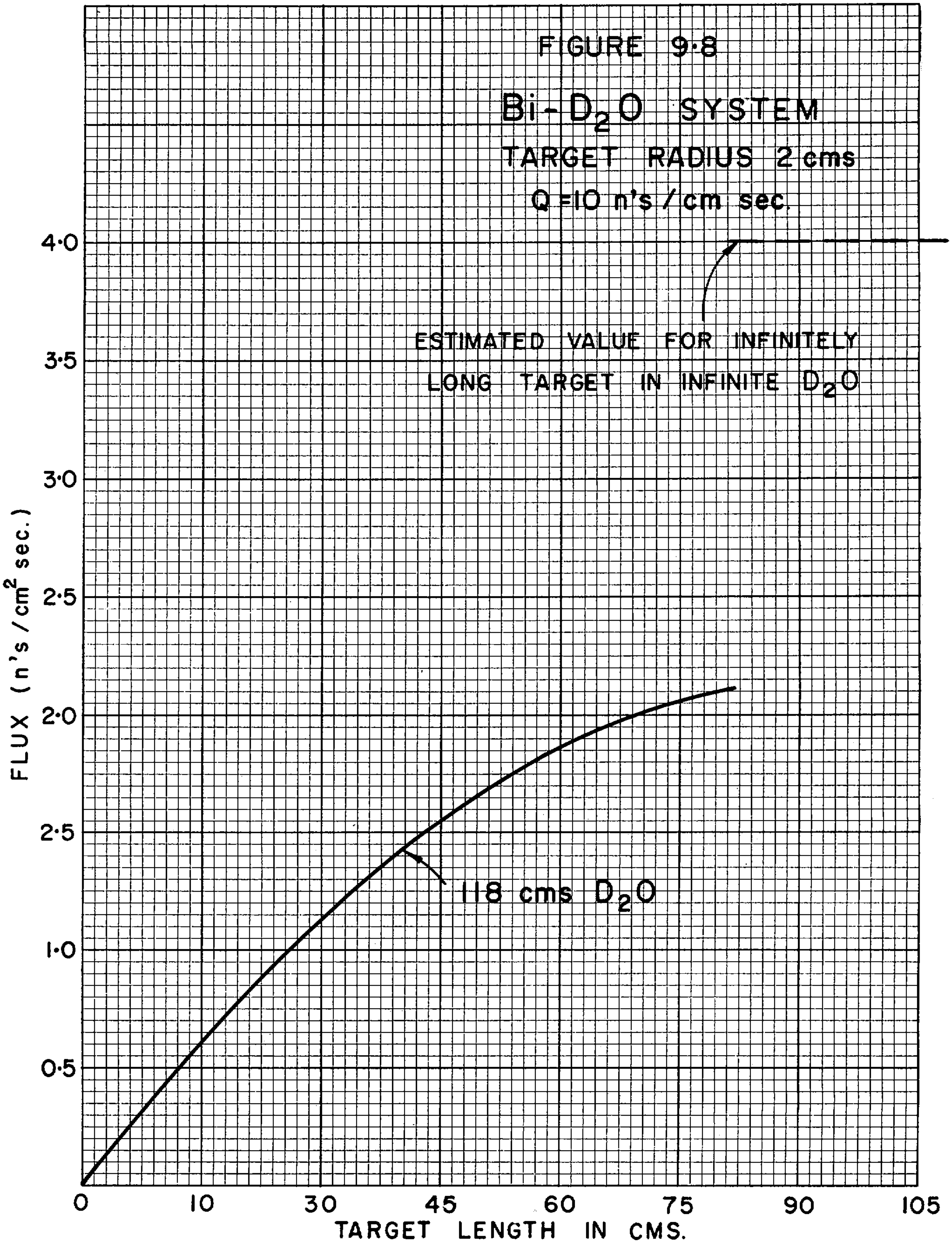

FIGURE 9·8
Bi - D_2O SYSTEM
TARGET RADIUS 2 cms
Q = 10 n's / cm sec.
ESTIMATED VALUE FOR INFINITELY LONG TARGET IN INFINITE D_2O
118 cms D_2O
FLUX (n's / cm^2 sec.)
4·0
3·5
3·0
2·5
2·0
2·5
1·0
0·5
0
10
30
45
60
75
90
105
TARGET LENGTH IN CMS.

4. REFERENCES

1. J.M. Hendrie and H.J.C. Kouts, TID 14771(1961).
2. J.M. Hendrie, A.N.S. Trans. 5, 424(1962).
3. Lennox, Barts, Batch, Beyer, Jorgensen, Kelber, Reed, Rezek, Rosenberg, Stevens and Weatherhead, ANL 6451 (1961).
4. L.W. Fromm, Research Reactor Fuel Element Conference, Gatlinberg (September 17-19, 1962) TID 7642(1962).
5. W.B. Lewis, "The Significance of the Yield of Neutrons From Heavy Nuclei Excited to High Energies", Atomic Energy of Canada Limited Report, AECL 968 (1952).
6. "Status of the MTA Process", Livermore Research Laboratory, LRL-102 (Del.) (1954).
7. "A Proposal for the Mc^2 Isochronous Cyclotron", Oak Ridge National Laboratory Report, O.R.N.L. 3540(1963).
8. T.E. Cole and A.M. Weinberg, An. Rev. Nuclear Sci. 12, 221 (1962).
9. L.W. Smith and P.G. Kruger, Phys. Rev. 83, 1137(1951).
10. Allen, Nechaj, Sun, and Jennings, Phys. Rev. 81, 536(1951) as re-assessed by J.L. Fowler and J.E. Brolley, Revs. Modern Phys. 28, 103(1956).
11. See for example Gaerttner, Yeater and Fullwood, I.R.E. Trans. Nucl. Sci. NS-9, 23(1962).
12. R. Bergere in "Neutron Time-of-Flight Methods", J. Spaepen ed., European Atomic Energy Community (EURATOM) Brussels, 329(1961).
13. See for example J.B. Adam, The New Scientist 31, 222(1963).
14. W.E. Crandall and G.P. Millburn, J. App. Phys. 29, 698(1958).
15. "A Progress Report on the Design of a Very High Intensity Linear Accelerator for Protons at an Energy of 750 MeV", Yale University Physics Dept. Internal Report Y6, T.I.D. 17766 (1962).
16. "A Combined Function Proton Linear Accelerator", V.W. Hughes and G.W. Wheeler, Yale University, Physics Department, Accelerator Design Study Group, (October 2, 1963).

17. D. Nagel, Invited Paper, American Physical Society, Chicago, October 19, 1963 and private communication from D. Nagel.

18. Livingston, Hudson, Jones, Lord, Mann, Martin, Russell, Ziegler, and Zucker, Nuclear Inst. and Methods, 18, 19, 438 (1962).

19. F.M. Russell "A Strong Focussing Cyclotron with Separated Orbits", ORNL 3431 (1963).

20. F.M. Russell and R.S. Livingston, Int. Conf. on High Energy Accelerators, Dubna, USSR, August 1963.

21. F.M. Russell, I.E.E.E. Summer General Meeting and Nuclear Radiation Effects Conference, Toronto, June 16-21, 1963.

22. J.C.D. Milton and J.S. Fraser, Bull. Am. Phys. Soc. 9, No. 4, 445, 1964 and to be published.

23. Bercovitch, Carmichael, Hanna and Hincks, Phys. Rev. 119, 412(1960).

24. F.M. Russell, private communication (1964).

25. Meadows, Ringo and Smith, Nuclear Inst. and Methods 25, 349(1964).

26. R. Wallace and C. Sondhaus, UCRL 10439 (1962), R. Wallace, Proc. Int. Conf. on Sector-Focused Cyclotrons, Los Angeles, April 1962, 405(1962).

27. B. Moyer, First International Conference on Shielding around High Energy Accelerators, Orsay and Saclay, January 1962, Presses Universitaires de France, 65(1963).

28. Metropolis, Bivins, Storm, Turkevitch, Miller and Friedlander, Phys. Rev. 110, 185(1958).

29. Metropolis, Bivins, Storm, Miller, Friedlander and Turkevitch, Phys. Rev. 110, 204(1958).

30. Dostrovsky, Rabinowitz and Bivins, Phys. Rev. 111, 1659(1958).

31. USAEC Annual Report to Congress of the AEC for 1962, 342, U.S. Government Printing Office, Washington, D.C., 1963.

32. K. Johnsen, Minutes of Conference on Linear Accelerators for High Energies, Brookhaven 1962, B.N.L. 6511, 267(1962).

33. Edge, Hughes and Sandweiss, Bull. Am. Phys. Soc. 9, 45(1964).

34. Bernardini, Bizzarri, Corazza, Ghigo, Querzoli and Touschek, Proceedings International Conference on High Energy Accelerators, Brookhaven 1961, TID 7636 (1961).

35. G.K. O'Neill, Proceedings of International Conference on High Energy Accelerators, Brookhaven 1961, TID 7636 (1961).

36. E.D. Courant, Brookhaven National Laboratory report BNL 7091, 34(1963).

37. A. Schoch, Nuclear Inst. and Methods 11, 40(1961).

38. B. de Raad, CERN report AR/Int. S.G./62-6(1962).

39. D. Reilly, MURA report MURA-477(1959).

40. E.J. Woods, Proceedings of International Conference on High Energy Accelerators, Brookhaven 1961, TID 7636(1961).

41. H.G. Herewood, discussion, Session VI, Storage Rings, Proceedings of International Conference on High Energy Accelerators, Brookhaven 1961, TID 7636, 287(1961).

42. H. Goldstein,'Classical Mechanics',Addison Wesley (1951).

43. Bernardini, Corazza, Di Giugno, Ghigo, Haissinski, Marin, Querzoli and Touschek, Phys. Rev. Letters 10, 407(1963).

44. G.K. O'Neill, International Conference on High Energy Accelerators and Instrumentation, CERN, 1959, 23,CERN Scientific Information Service, Geneva, Henri Studer (1959).

45. A. Michaudon, Reactor Science and Technology, 17, 165(1963).

46. J. Rainwater, 'Neutron Time-of-Flight Methods', J. Spaepen, ed., 321 EANDC (1961).

47. Blokhin, Blokhintsev, Blyumkina, Bondarenko, Deryagin, Zaimovskii, Zinov'ev, Kazachkovskii, Kim Khen Bon, Krasnoyarov, Leipunskii, Malykh, Nazarov, Nikolaev, Stavisskii, Ukraintsev, Frank, Shapiro, and Yazvitskii, Atomnaya Energiya 10, 437(1961). English trans. Sov. J. of Atomic Energy 10, 430(1962).

48. G.J. Neary and J. Mulvey, Paper HL 59/6932, PIRC-HP17, Medical Council Radiobiological Unit, AERE, Harwell.

49. S.J. Lindenbaum, Proceedings of First International Conference on Shielding around High Energy Accelerators, Presses Universitaires de France, 43(1962).

50. M. Baarli, Proceedings of First International Conference on Shielding around High Energy Accèlerators, Presses Universitaires de France, 123(1962).

51. Wolfgang, Baker, Caretto, Cumming, Friedlander and Hudis, Phys. Rev. 103, 394(1956).

52. Belyaev, Kalyamin, and Murin, Izv. Akad. Nauk S.S.S.R., Ser. Fiz. 27, 923(1963).

53. J.M. Dickson, Proceedings of International Conference on High Energy Accelerators, Brookhaven, TID 7636, 363(1961).

54. 'Information Relevant to the Choice of the Primary Proton Energy for a Meson Factory', Edge, Hughes, Knowles and Ohnuma, Yale University Internal Report Y-8, March 16, 1964.

55. R.L. Gluckstern, Conference on Linear Accelerators for High Energies, Brookhaven National Laboratory BNL 6511, 124(1962).

56. M. Roos, Revs. Modern Phys. 35, 314(1963).

57. S. Kushneriuk, A.E.C.L. report to be published.

Additional copies of this document
may be obtained from
Scientific Document Distribution Office
Atomic Energy of Canada Limited
Chalk River, Ontario, Canada

Price - $3.00 per copy